STUDY OF FLUORESCENCE PHOTOBLEACHING AND RECOVERY OF HUMAN BREAST TISSUES AND TISSUE PHANTOMS

By

BHAWNA

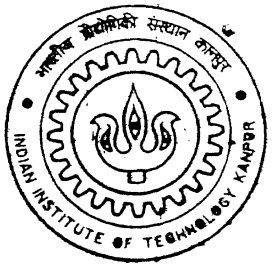

CENTER FOR LASER TECHNOLOGY

Indian Institute of Technology Kanpur

MAY, 2002

STUDY OF FLUORESCENCE PHOTOBLEACHING AND RECOVERY OF HUMAN BREAST TISSUES AND TISSUE PHANTOMS

A Thesis Submitted

in Partial Fulfillment of the Requirements

for the degree of

MASTER OF TECHNOLOGY

by

BHAWNA

to the

CENTER FOR LASER TECHNOLOGY
INDIAN INSTITUTE OF TECHNOLOGY
KANPUR-208016 INDIA

MAY, 2002

Dedicated
to
my parents

CERTIFICATE

It is certified that the work contained in the thesis entitled *"Study of Fluorescence Photobleaching and Recovery of Human Breast Tissues and Tissue Phantoms"*, by Miss. Bhawna, has been carried out under my supervision and that this work has not been submitted elsewhere for a degree.

Asima Pradhan
Asst. Professor
Laser Technology Programme
I.I.T. Kanpur 208016

May 2002

Contents:

ABSTRACT

In this thesis attempts have been made to differentiate normal, benign and malignant tumors of human breast tissues by using the techniques of Fluorescence Recovery After Photobleaching (FRAP). Changes in the fluorescence intensity at 530 nm and 630 nm are measured as a function of incident intensity with visible wavelength 488 nm excitation of Argon ion laser. The major emphasis is on flavin and porphyrin molecules within the tissues, which are fluorescent with 488nm excitation. Human breast tissues were obtained after surgical resections.

A theoretical model to obtain the variation of fluorophore concentration inside the tissue is developed from previous reports. Validity of these results is then correlated with phantom studies and tissue dynamics. The kinetics of fluorophores inside the tissues and in solutions is thus looked into and their behaviour studied. This model shows us that, besides the single or double exponential term in the decay or growth profile, there is a term that may enhance the ongoing process or make it compete with the other process to give either of the processes, recovery and bleaching respectively or both simultaneously.

Photobleaching curves of normal and diseased tissues display double exponential behaviour with different decay rates. Photobleaching rates of fluorophores in solutions mostly display single exponential behaviour while addition of absorber and scatterers results in double exponential profiles. The decay profile of FAD + Protoporphyrin indicates the contribution of both fluorophores in tissue photobleaching at 530 nm. Photobleaching profiles of normal tissues with blood show a fast decay in comparison to the normal and diseased tissues without blood. The fast decay rates of tumors indicate absorption of flavin by porphyrin. Fluorescence photobleaching recovery (FPR) profiles of tissue displays single exponential behaviour but the rates of growth of normal and diseased tissues are different.

There may be different reasons for FRAP recovery process as is discussed in this thesis. The study indicates that, FRAP is due to diffusion of fluorophores across the illuminated region and not necessarily due to reversible chemical reactions or due to some photoproduct formation. Though future work are required for conclusive results, this is just the first step towards understanding the mechanisms involved.

ACKNOWLEDGEMENTS

I would like to take this an opportunity to express my deepest gratitude to my thesis supervisor Dr. Asima Pradhan for introducing me to this exciting field of biomedical applications of laser. Her immense patience, endurance and meticulous handling of problems encouraged me and made me stay worthwhile at the institute. She has been a perennial source of inspiration and information for me. I am an indeed fortunate one to get an opportunity of working with her.

With pleasure I thank Dr. A.Agarwal and Dr. A.Rastogi, Dr. S.Swain, G.S.V.M. Medical College, Kanpur for their valuable suggestions and for providing the biological samples used in the present study.

Special thanks to Mayadi and Sharad for their constant help during the experiments and analysis of data. I also acknowledge the immense co-operation and lively company that I have received from my lab mates, Santosh, Tuhin and Pallab. I am also thankful to all the staff members of CELT office and workshop.

I shall remain indebted to my parents for their constant support, inspiration and understanding without which I wouldn't be what I am today. It is a pleasure to thank my sister Anshu for her love, affection, help, constant moral support and active assistance during many phases of life.

List of Figures

List of Tables

CHAPTER 1

Introduction

1.1 Introduction

Lasers are used in medicine and biology in various applications. Historically, the thermal effects of lasers have been mostly of importance especially in therapy. In recent times, laser spectroscopy plays a dominant role in number of applications. Lasers are well known in surgery as effective cutting tools. The penetration depth of laser light in tissue is largely determined by the absorption properties of water, hemoglobin and skin pigment melanin as well as by the highly scattering effects.

Research and development of application-specific lasers have changed the practice of dermatology by allowing vascular lesions, pigmented lesions, tattoos, and hair to be removed without scarring. These important examples of selective photothermal injury are being refined and extended. More importantly, the potential for laser applications in skin diagnosis, imaging, and treatment for burns far exceeds their present use. A detailed understanding of skin optics, photothermal, and photoacoustic processes is emerging. Innovative schemes for delivery and control of laser irradiation, including robotics, can potentially improve therapy. Laser spectroscopy and imaging techniques hold significant diagnostic promise in dermatology.

Although spectroscopic aspects in terms of absorption properties do play a role in photothermal and photoablative treatment, laser spectroscopy is equally important in the fields of laser photodynamic therapy and tissue diagnostics using laser induced fluorescence (LIF). LIF studies are performed in a regime where no change in the tissue is induced by the lasers. It is proven to useful for diagnostic purpose [1].

On absorption of electromagnetic radiation, the pathways of a molecule back to the ground state are affected by its inherent structure and the physiochemical properties of its local environment. The pathways back to the ground state involve emission of electromagnetic radiation and when this emission is from a singlet state the process is called fluorescence. Fluorescence is unique among spectroscopic technique because it is multidimensional [2]. The emission process contains a wealth of information that is related to the fluorescence and its surroundings. Several groups have been investigating the use of fluorescence for possible cancer diagnosis and promising results have been achieved [3-6]. There exists considerable interest in the use of laser-induced fluorescence from native tissues for discriminating cancerous and precancerous tissues from benign tumors and normal tissues [7]. This is because of sensitivity of this process and the time scales in which this occurs.

A brief description of fluorescence follows:

1.2 Fluorescence

Luminescence is the emission of photons from electronically excited states, and can be classified as bioluminescence, chemiluminescence, and photoluminescence by means of energy supplied to excite the molecules. When molecules are excited by interaction with photons and return to ground state by emission, the process is called photoluminescence. In fluorescence spectroscopy, molecules are excited to an activated state and undergo subsequent relaxation by a non-radiative decay and then to ground state or by a decay which results in a fluorescent photon with a lifetime of 10^{-12} - 10^{-9} seconds.

A wide range of molecular processes such as absorption, fluorescence, phosphorescence, Raman effects can occur during this time period and these are reflected in the spectral profile of the fluorescing compound. Hence, it is being increasingly used in biomedical and chemical research. The absorption and emission of light by the energy level diagram is shown in figure 1.1

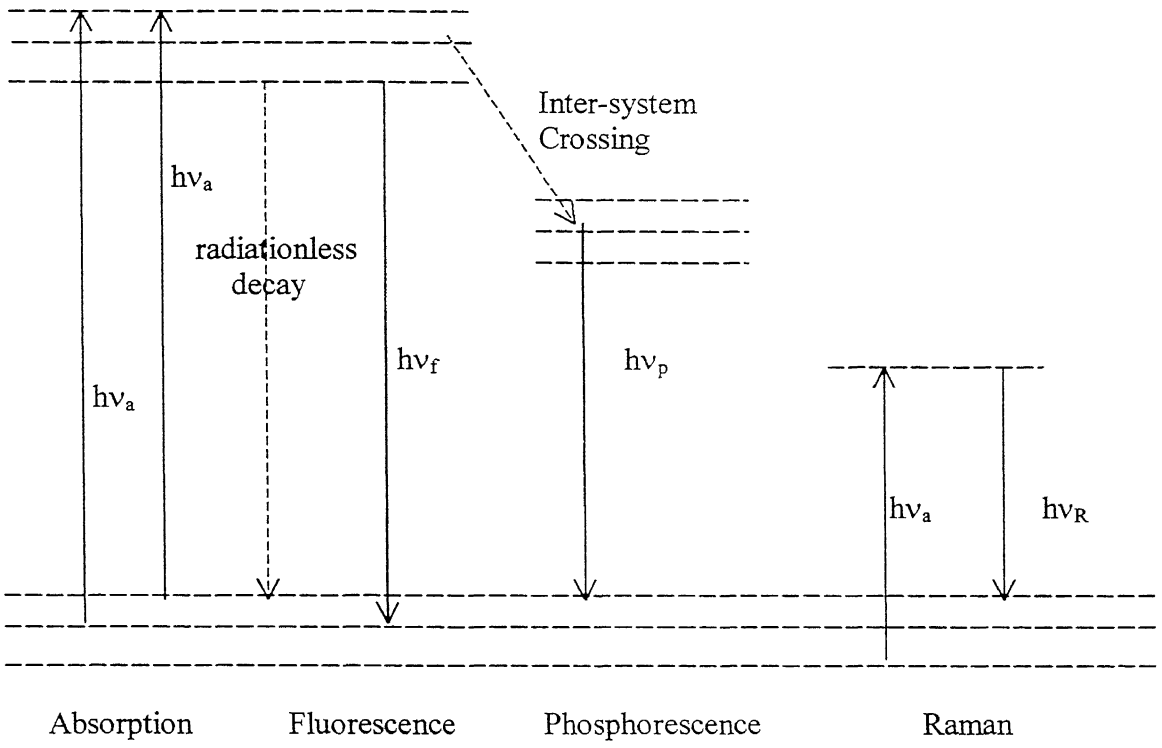

Figure 1.1 The energy diagram for the electronic and vibrational energy transitions associated with absorption, fluorescence, phosphorescence and Raman spectroscopies.

The key parameters in the study of fluorescence are: λ_{em} – the position of maximum emission intensity, λ_{ex} – the excitation wavelength, φ - the quantum yield and τ_f – the fluorescence relaxation time. These parameters are very sensitive to change in the environment of the fluorophore, and specifically of fluorophores in tissues, in this study. For example, an increase in cell density of the tissues causes more non-radiative losses and due to this effect, emission lifetimes will change.

Fluorescence can be divided into static and dynamic forms. These categories can be further divided into sub categories with different features.

Static fluorescence

1) In static spectroscopy, the intensity of the profile tells us about the concentration of molecules or fluorophores, quenching of fluorophores due to molecular accessibility, conformational changes.
2) The spectral profiles provide information on the local environment surrounding the fluorophores (e.g. polarity, pH), the number of emitting components.
3) The polarization spectroscopy or anisotropy measurements tell us about the average size of a rotationally mobile species, mobility or motional restriction, binding of molecule, density of molecules.

The tools used may be

a) **Steady state fluorescence spectroscopy**

Steady state fluorescence spectroscopy is a useful tool to diagnose biological samples, where the excitation wavelength is fixed and the emission wavelength is scanned to obtain a fluorescence spectrum

b) **Excitation fluorescence spectropscopy**

Excitation spectroscopy is a useful tool to investigate medical and biological samples to identify the emitting species. The excitation spectrum is determined from the measurement of the intensities at a selected fluorescence wavelength as a function of the excitation wavelength and in general follows the absorption curve.

c) **Synchronous spectroscopy**

Here the excitation and emission wavelength are both varied. The spectrum obtained is basically a convolution of absorption and emission spectra of the sample. This method gives higher resolution as compared to other spectroscopy methods.

Dynamic or time resolved fluorescence

1) Excited state intensity decay provides information about the contribution of the individual emissive centers, continuous lifetime distributions.
2) Decay of polarization anisotropy gives additional information about the diffusive motion of the fluorophore, rotational motion (i.e., if the environment restricts its angular displacements).

Tools used are:

Time resolved fluorescence

Samples are excited by an optical pulse, which is much shorter than the lifetime of the excited state of the samples. The fluorescence intensities at different wavelength can be measured as a function of time.

1.3 Advantages and Limitations of Fluorescence

The advantages of molecular emission (fluorescence and phosphorescence) are (a) excellent sensitivity, (b) good specificity. Fluorimetric methods can detect concentrations of substances as low as one pare in 10 billion, a sensitivity 1000 times greater than that of most spectrophotometric methods. This increased sensitivity is because in fluorescence the emitted radiation is measured directly and can be increased or decreased by altering the intensity of the exciting radiant energy. An increase in signal over a zero background signal is measured by fluorimetric methods. With spectrophotometric methods the analogous quantity, absorbed radiation, is measured indirectly as the difference between the incident and transmitted beams. This small decreased in the intensity of a very large signal is measured in spectrophotometry with a correspondingly large loss in sensitivity. All the net fluorescence signal might be the same as in absorbance spectroscopy, the emission can be amplified many times to give great sensitivity of analysis.

The specificity of fluorescence is the result of two main factors: (a) there are fewer fluorescent compounds than absorbing ones because all fluorescent compounds must necessarily absorb radiation, but not all compounds that absorb radiation emit. In fact,

only 10% of all absorbing compounds will emit radiation via luminescence. (b) two wavelengths are used in fluorometry, but only one in spectrophotometry. Two compounds that absorb radiation at the same wavelength will probably not emit at the same wavelength. Likewise, two compounds that emit at the same wavelength will probably not absorb at the same wavelength.

Because of its sensitivity to environment, fluorescence is mostly affected by the temperature, pH and ionic strength etc., which is the major disadvantage. Quenching is another serious problem, but the analysis of various quenching processes may provide important information about the dynamics of collision between the fluorophore. These are several types of quenching observed in luminescence that is temperature, oxygen, concentration and impurity quenching. The fluorescence of a compound is affected by the viscosity of the medium, increasing with increasing viscosity. Energy transfer is reduced by a reduction in the number of molecular collisions. Thus, the fluorescence of most compounds can be increased by using a more viscous solvent such as glycerol or gelatin.

1.4 Fluorescence Recovery After Photobleaching (FRAP)

The temporal decrease of fluorescence signal is normally referred to as photobleaching process. Initially, when light is incident on the sample, very few molecules exist in the excited state. Hence, a large number of molecules present in the ground state absorb the incident radiation and fluorescence intensity is high. However, with time, more and more molecules get excited and very few are left in the ground state.

This is known as ground state depletion or bleaching and results in a drop of the emitted fluorescence intensity. Alternately, the irradiated fluorophores are photochemcially may be altered and unable to fluoresce anymore. The fluorophore may be reversibly altered, leading to recovery of fluorescence. Recovery may occur due to diffusion of fluorophores into the irradiated area.

FRAP is based on the principal of observing the rate of recovery of fluorescence signal either due to the movement of fluorophores into an area of the tissue which has been rendered non-fluorescent via an intense laser light of appropriate wavelength or due to some irreversible chemical reactions occurring leading to the formation of some photoproducts, thereby reducing the concentration of loopholes of the medium. The recovery is monitored by an attenuated beam just after the photobleaching.

FRAP is nowadays being used to measure the lateral diffusion of various membrane or cytoplasmic constituents. Graphical representation of FRAP process is shown in figure 1.2. A baseline of fluorescence is collected (1) before the photobleaching occurs (arrow) so that the amount of fluorescence is reduced significantly (2). Over time, the amount of fluorescence in the photobleached area increases as unbleached molecules diffuse into this area (3). Later there is a stabilization of the amount of fluorescence recovery (4) and a flat line is obtained. The formula for percent recovery is given as: X- (X-Y)=% recovery. In this diagram the percentage of fluorescence lost due to photobleaching is X and the amount of fluorescence that returns to the bleached area is Y. In practice, the percent recovery rarely reaches 100%. The lateral mobility is determined by the slope of the curve (3). The steeper the curve, the faster the recovery and therefore, the more mobile the fluorophores.

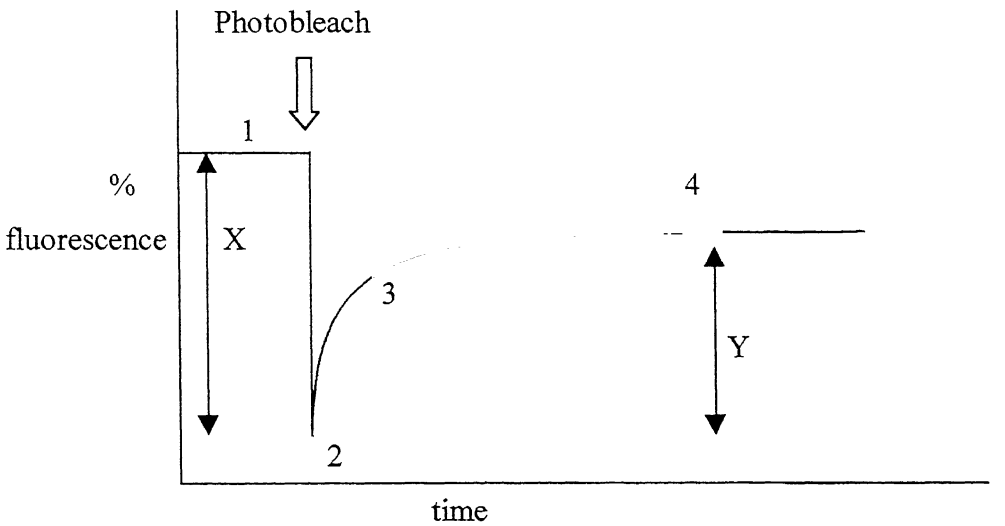

Figrue 1.2 Graphical representation of FRAP process

1.5 Biological tissue

Tissue is a group of cells organized to perform a specialized function. Understanding the propagation and the distribution of light in biological tissues is important for safe use in medical diagnostics [9]. Biological tissue is an optically turbid medium and normally contains several fluorescing compounds, such as flavin, nucleotides (NADH), tryptophan, tyrosine, elastin, collagen etc [8]. Flavins are intrinsic fluorophores emitting in visible region. Flavin adenine dinucleotide (FAD), flavine mononuceotide (FMN) and free riboflavin are the three forms of riboflavin encountered in biological materials. These flavins may be attached to proteins or may be free. These are coenzymes that play a role in oxidation-reduction process of the tissues. Hence, they may play a major role in triggering tumor growth [10].

Diseased tissue differs from normal tissue morphologically. However, disease may occur only with subtle visible changes. Cancer is a disease characterized by the uncontrolled growth and spread of abnormal body cells. The human body is made up of billions of cells. Normally, cells reproduce themselves by dividing so that growth occurs.

Worn out tissues are replaced and injuries are repaired in this manner. Occasionally, cells abnormally grow into a mass called a tumor. Some tumors are benign (non-cancerous); others are malignant or cancerous.

The growth of benign tumors may interfere with body function, but these tumors are seldom life threatening. Malignant tumors, on the other hand, invade and destroy normal tissue. by a process called metastasis, cell breaks away from a cancerous tumor and spreads through blood and the lymphatic system to other parts of the body where they form new tumors. Sometimes, cancer grows and spreads rapidly. In other cases, it develops and spreads slowly.

Breast cancer

Breast cancers are characterized as malignant because they have the ability spread, or metastasize, and cause death. Although doctors, nurses, patients and everyone else tends

to talk about breast cancer like it is one disease, in reality there are numerous types of breast cancer. Some are only modestly malignant while others are extremely serious. Obviously the treatment with these two different types of breast cancer would be different as well. Furthermore, each type of breast cancer will be diagnosed in some stage of the disease, meaning that two woman with the same type of breast cancer may have different treatments and a different prognosis because one is more advanced than the other. And finally, there are a whole host of non-cancerous (benign) breast diseases as well [11].

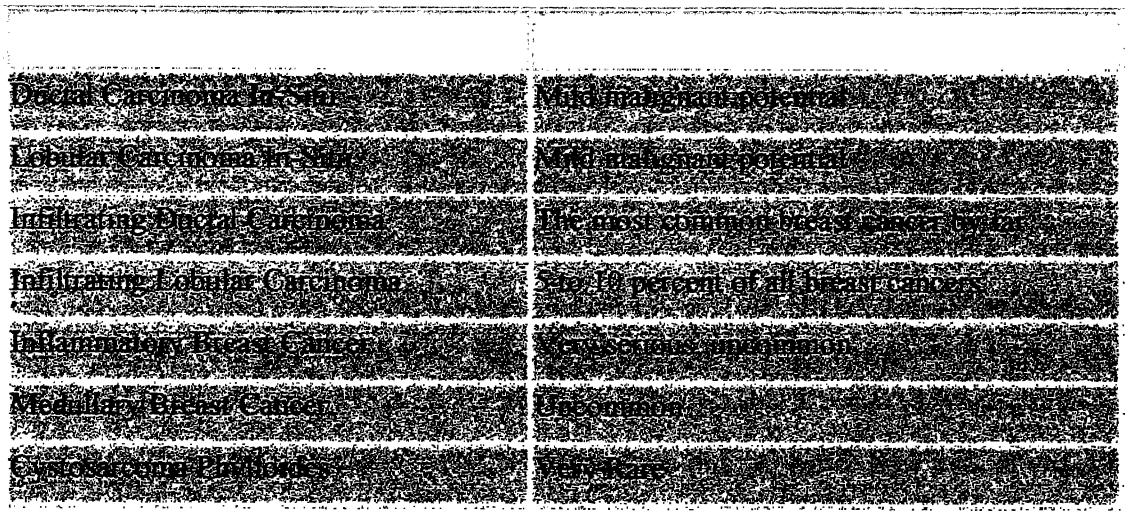

Breast tumors studied in this research were generally infiltrating ductal carcinomas.

1.6 Focus of the thesis

Optical spectroscopy has potential to differentiate the bio-chemical and morphological changes of normal and diseased tissues. Photobleaching is a dynamic process under which fluorophores become inactive in the presence of light. This photo-induced "killing" of fluorophores causes the loss of fluorophores in excitation and emission processes. The rates of photobleaching are dependent upon the intensity of

incident light and exposure time. To know the exact mechanism of photobleaching one has to study the medium where concentration and environment of participating

molecules are well controlled. The photobleaching profiles of human tissues have been earlier observed to have double exponential behaviour. There may be different reasons for this higher order behaviour in tissues. It can be due to the presence of two fluorophores, some photoproduct formation, damage of cell membrane, flow through membrane or oxidation-reduction process of fluorophores. So, study of photobleaching and fluorescence recovery may offer us a method of understanding biochemical and environmental changes in cells and tissues and can discriminate between normal and

diseased tissues. However, mechanism of its temporal dynamics is not yet well known enough. The focus of the thesis is to study fluorescence photobleaching and recovery in human breast tissues in this report. The effects of exposure time and irradiation intensity have been looked into and correlation with various phantom solutions is discussed.

1.7 Thesis Organisation

The second chapter describes the experimental set-up used to study the photobleaching and recovery of human tissues. Third chapter discusses the dependence of photobleaching and recovery on various parameters like exposure time and irradiation intensity, excitation wavelength etc. Fourth chapter gives the mathematical model for photobleaching and recovery. Finally, the last chapter deals with conclusion and future aspects.

1.8 References

1. R.R.Alfano, B.T.Darayash, J.Cordero, P.Tomashafsky, F.W.Longo, M.A.Alfano, "Laser induced Fluorescence spectroscopy from Native cancerous and normal Tissues", IEEE Quantum Elect. 20: 1507 (1984)

2. J.R.Lakowicz, Principles of fluorescence spectroscopy, (1983)

3. C.C.Hoyt, R.R.Richards Kortum, B.Costells, B.A.Sucks, C.Kittrel, N.B.Ratliff, J.R.Kramer and M.S.Feld, Laser surg. Med., 8:1(1988)

4. R.Richards Kortum, A.Mehta, G.Hayes, R.Cothren, T.Kolubayer, C.Kittrel, N.B.Ratliff, J.R.Kramer and M.S.Feld, Amer. Heart J., 118:381(1989)

5. R.Alfano, B.B.Das, E.Celmer, R.Prudente, J.Clearly, "Light sheds light on cancer distinguishing malignant tumors from benign tissues and tumors, Bull. N.Y.Acad. Med., 67: 143 (1991)

6. G.C.Tang, A.Pradhan, W.L.Sha, J.Chen, C.H.Liu, S.J.Wahl and R.R.Alfano, "Pulsed and cw laser fluorescence spectroscopy from cancer and chemically treated normal breast and lung tissues", Appl. Opt., 28: 2337 (1990)

7. R.Richards Kortum and Sevick-Muraca E., :Quantitative optical Spectroscopy for tissue diagnosis". Annu. Rev. Phys. Chem., 47: 555-606 (1996)

8. A.Pradhan, "Fluorescence spectroscopic properties of Normal and Abnormal Biomedical Materials", Thesis City University of New York (1991)

9. M.S.Patterson, B.C.Wilson and D.R.Wyman, "The Propagation of Optical Radiation in tissues", Laser Med. Sci.,6: 155 (1991)

10. S.Ghisla, V.Massey, J.Lhoste and S.G.Mayhew, "Fluorescence and Optical Characteristics of reduced Flavins and Flavoproteins", Bio-Chem, 13: 589 (1974)

11. A.Rastogi, "Evaluation of various Diagnostics Modalities in Breast Lesions with special reference to role of Laser Spectroscopy", Thesis in S.S.M. Kanpur University.

CHAPTER 2

Experimental Aspects

2.1 Introduction

The successful application of a spectroscopic method requires an understanding of its instruments. Considerable attention to the experimental details is therefore necessary. In this chapter the experimental set up for the emission spectra is described in detail.

Absorption and emission polarization spectroscopy has served as useful tools for identifying fluorophore electronic states and conformational structure in different environments. The harmful effects of X-rays and nuclear radiation have forced scientists to resort to other techniques such as Ultrasonography, immune diagnosis, computed tomography and imaging tissues. Fluorescence spectroscopy is a recent development in this category growing very fast [1].

The description of the instrumentation involved in the photoluminescence spectroscopic is described here. The primary instrument in use is an Argon ion laser cooled by the chiller plant, the spectrometer for dispersion of light and the photomultiplier tube (PMT) for detection, which are briefly described in this chapter.

2.2 Experimental Set-up for FRAP

The block diagram of the experimental set up used for the measurement of photobleaching and recovery profiles from normal and tumor human breast tissues have been shown in figure 2.1 [2]. The samples were excited with unpolarized argon-ion laser light operated at 488nm with ~20mW power at the sample site (power at the source is 100mw). Any fluctuation in the laser power was less than 0.3%. The laser light was focused onto a spot size of nearly 10μm on the front surface of the tissue. The fluorescence was recorded using a SPEX-1877E triplemate blazed at 500nm and cooled Photomultiplier tube (PMT). The output of the detector was connected to a computer for data acquisition and analysis.

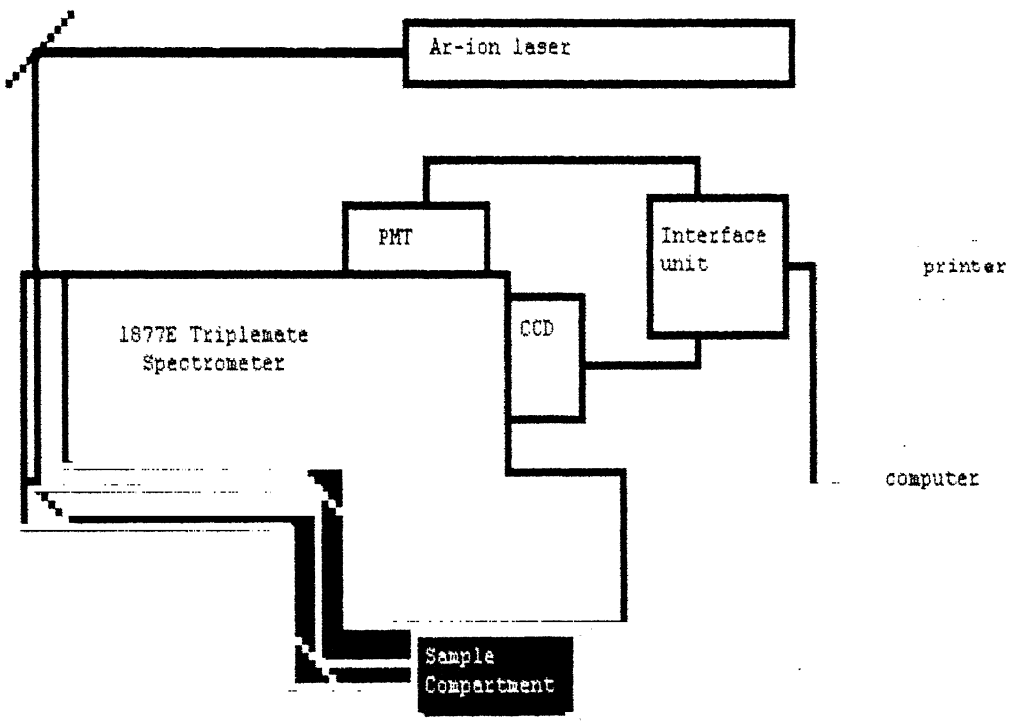

Fig. 2.1 Schematic diagram of the Experimental setup

• 5 Watt Ar-ion Laser

Spectra Physics model 165 Ar-ion laser mainly consists of a laser head and 265 exciter. The laser head consists of a plasma tube of Beryllium oxide (both ends are enclosed by Brewster's angle windows), a solenoid and an optical resonator. Power output is 5W laser. The resonator consists of a spherical mirror at the output end and a prism assisted by a flat mirror at the back end. The 265 exciter contains all the electronics required to drive the laser.

• Cooling system for Ar-ion laser

Ar-ion laser requires cooling for the transistor bank in the exciter, magnetic field solenoid and the plasma tube. Neslab chiller plants have been used for the cooling. The chiller plant mainly consists of reservoir, temperature controller, re-circulating pump, and a refrigeration unit. The chiller plants supplies a constant flow of water at constant temperature of 22.5°C and 30 psi pressure to keep the laser cool. The cooling capacity of this plant is 15.7kW.

• Spectrometer (SPEX1877-triplemate)

Raman monochromators are specially designed to provide low stray light and flat specially tailored to provide the above specifications successfully [3]. The triplemate has two major sections i.e. the filter and spectrograph stages. The filter stage consists of two modified Czerny-Turner 50 mm x 50 mm plane gratings having 600 grooves/mm, coupled in a subtractive mode, and giving a bandpass of about 1000 cm^{-1} on a 5 mm intermediate slit setting. The focal length of the stage is 0.22 m. It acts as a variable wavelength, selectable bandpass filter that feeds a non-dispersed segment of radiation from a sample into the entrance slit of spectrograph stage. The spectrograph stage is a 0.6 m, single monochromator which disperses the radiation over the detector. It consists of an asymmetric Czerny-Turner mount with 64mm x 64mm plane grating having 1200 grooves/mm and is used to produce a dispersion of 1.4 nm/mm. To vary the dispersion and coverage at the focal plane, the spectrograph has provisions for mounting three

gratings of different groove densities on a manually activity turret. The dispersed radiation is then detected by a thermoelectrically cooled PMT. The optical path of the triplemate is shown in Figure 2.2 and the specifications of the triplemate are given in Table 2.2.

Light passes into the entrance S1 collimated by M1 onto G1 where it is dispersed onto M2. After passing through S2, which determines the bandpass of the filter stage, the light strikes the spatial-filter mirror (M3) and passes through a fixed slit, which eliminates much of the stray light. Again the light is collimated (M4) dispersed (G2), in an opposing direction to cancel the effects of the internal dispersion, then focused (M5) onto the exit slit of the filter stage (S3) which controls the resolution of the spectrograph stage, in this final stage the light is again collimated (M6) and dispersed on whichever of the turreted gratings (G3) is selected. The camera mirror (M7) projects a flat image onto the focal plane where it is seen by the detector.

Table2.1: Characteristics of SPEX 1877 E Triplemate

Element	**Specifications**	
	Filter Stage	**Spectrograph Stage**
Mount (Czerny-Turner)	Two, subtractive mode	Asymmetric
Focal Length	0.22 m	0.60 m
Gratings	50 x 50 mm^2	64 x 64 mm^2
Grooves/mm	600	1200/1800
Dispersion at 514.5 nm		1.44 nm/mm
Spectra range	185-1000 nm	54,000 – 10,000 cm^{-1}
Accuracy	± 0.5 nm	± 0.5 nm

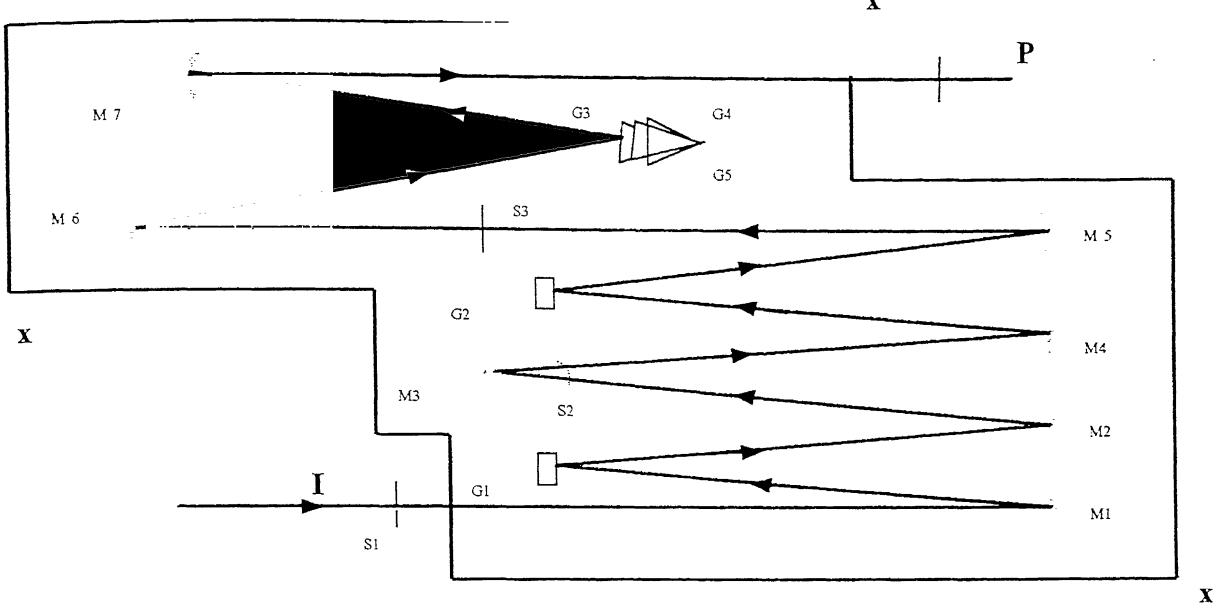

x: Position of metal leg, G: Grating, S: Slit, M: Mirror, P: PMT, I: Laser Beam

Fig. 2.2 Optical path of triplemate Spectrometer

• Photomultiplier tube (PMT)

The PMT is a photosensitive device consisting of a photoemissive cathode followed by focusing electrodes, an electron multiplier and an electron collector in a vacuum tube. When light enters the photocathode, the photodiode emits photoelectrons into the vacuum. These are then directed by the focusing electrodes voltages towards the electron multiplier where electrons are multiplied by the process of secondary emission. The multiplied electrons are then, collected by the anode as an output signal. The PMT is supplied a high voltage of 1650 volts.

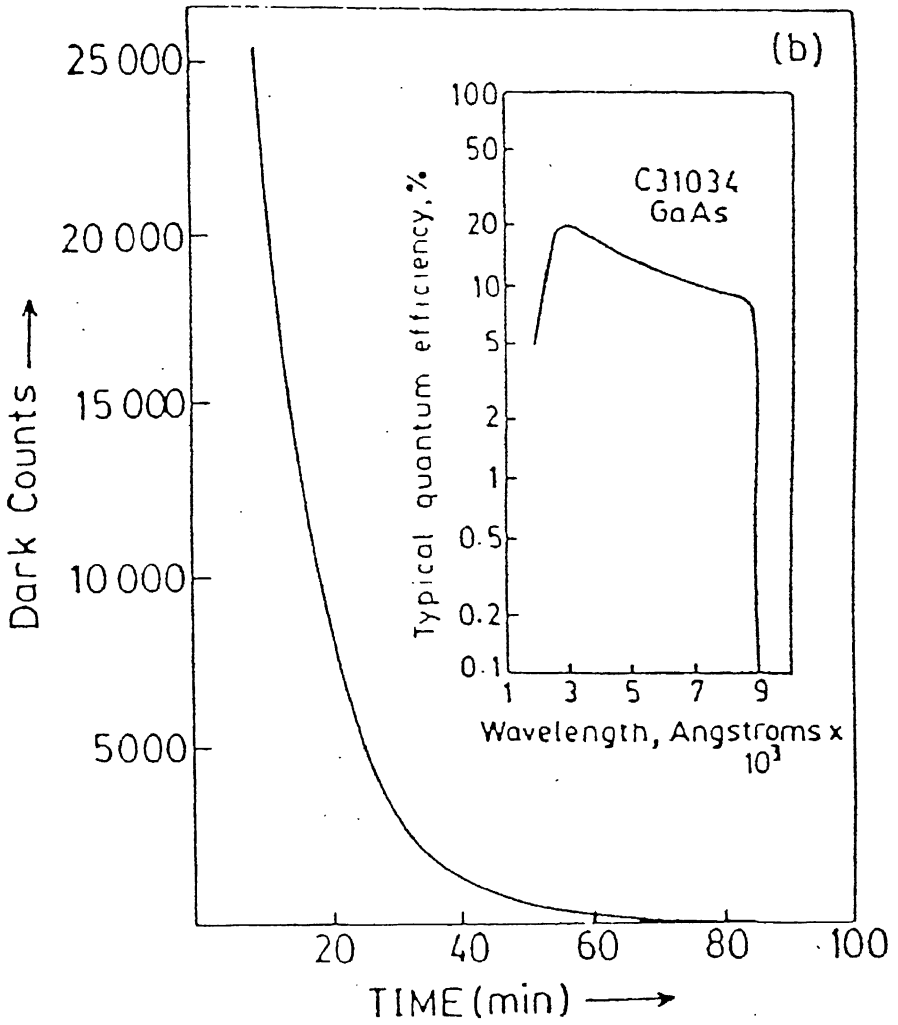

Fig. 2.3 Dark current-vs-time curve after switching on the thermoelectric cooling of PMT. The inset shows quantum efficiency of PMT with wavelength.

2.3 References

1. Fluorescence Diagnosis and photochemical treatment of diseased tissue using Laser – Part I, Analytical Chemistry, Vol.62, 1 (Dec15, 1989)

2. Sharad Gupta, Bhawna, Asima Pradhan, "Fluorescence Photobleaching and Recovery of Human Breast Tissues and Tissue Phantoms", SPIE Proceedings Vol.4613 (2002)

3. Operation and maintenance Instructions, 1877E Triplemate (Spex Industries Inc. USA).

CHAPTER 3

Fluorescence Photobleaching And Recovery Of Human Breast Tissues and Tissue Phantoms

3.1 Introduction

Photobleaching is a dynamic process in which fluorphores undergo photo-induced chemical destruction upon exposure to light and thus lose their ability to fluoresce. These bleached molecules can no longer take part in the excitation-emission cycle. Recovery is the increase of fluorescence signal just after photobleaching when monitored in an attenuated power. The rate of photobleaching is a function of excitation intensity. However, the mechanism of photobleaching in biological systems is not well understood due to the complexity of the heterogenous fluorophores and their environments. Almost all the existing knowledge on photobleaching comes from spectroscopic studies of fluorophores in solution, where the chemical environment is well controlled.

Fluorescence Photobleaching Recovery (FPR) is a common technique used in Photodynamic therapy (PDT) to calculate the lethal light dose required to destroy tumor cells without affecting the normal ones. PDT is the combination of light and light sensitive agents (such as porphyrins) in an oxygen-rich environment. Porphyrins are a component of hemoglobin, which in turn is a component of red blood cells. Hemoglobin

is what carries oxygen in the blood. When porphyrins are present in a form other than hemoglobin, they can absorb energy from photons (particles of light) and transfer this energy to surrounding oxygen molecules. Toxic oxygen species such as singlet oxygen and free radicals are thus formed. These chemicals are very reactive and can damage proteins, lipids, nucleic acids and other cellular components. Just as chlorophyll in plants utilizes energy from sunlight to produce sugar, porphyrins utilize energy from light to produce toxic oxygen species. In PDT, drugs known as porphyrins are administered intravenously into the body to sensitize diseased tissue to visible light. The affected tissue is then exposed to laser light in order to activate the porphyrin drug and cause chemical reactions in the tissue. The net result is selective tumor destruction. Several different drugs have been developed for PDT, but porfimer sodium (Photofrin) is the only drug that has received official approval for routine use in patients, and only then for the treatment of certain cancers. In recent times, FPR has been seen to be useful in extracting information from cells and tissues.

FPR is also a very powerful technique for study of lateral mobility of membrane lipids and proteins and to measure the rates of diffusion of specific components in cells across the cell membrane. Currently, there is widespread interest in this problem because of the apparent role of lateral membrane transport as indicator of changes in the physiological state and in the environment of cells and tissues. A mathematical model was given by D.Axelrod et al. in 1976 [1] to calculate the fraction of mobile flourophores in tissues and there by finding the diffusion rate and diffusion coefficient. In 1998, Teck-Chee-Chia and his co-workers used photobleaching phenomena in tissues as a diagnostic tool. Changes in autofluorescence intensities at 550nm, 580nm, 680nm and 720nm as functions of incident intensity and exposure time were measured in normal mucosa and adenocarcinomatous sites of human colonic tissues [2] when excited by the wavelengths of 457.9, 488, 514.5 and 632.8nm, respectively. The obtained results showed that there exists a difference in the decay rates between normal mucosa and adenocarcinoma of human colonic tissues. In 2000, Alexander A.Stratonnikov et al. extended their research on photobleaching and recovery and tried to explain fluorophore kinetics inside the tissues with a mathematical model [3]. However, very weak recovery has been observed by them. As per our knowledge, no other studies on fluorescence recovery has been done or observed in tissues. In this chapter bleaching and recovery has been observed in most of the tissues and

study has been carried out systematically on human breast tissues as a function of incident intensity and exposure time.

Tissues studies have been correlated with phantom studies to get an insight of the physical processes occurring during bleaching and recovery by studying the scattering and absorption effects. Cell membrane controls the flow of fluorophores and other molecules across it. On interaction with light some channels are formed in its layer, which provides motion for particular molecules and ions and restricts the motion for others. Further, studies may throw light into this mechanism playing a role in differences observed between normal and tumor decay rates. Photobleaching and recovery also provide us with a useful method to diagnose the disease at an early stage [1, 4]

3.2 Materials and Methods

Human breast tissues were obtained after surgical resections. Experiments were done on the same day of surgery and without any chemical treatment. A portion of tumor and its normal counterpart were taken to study the photobleaching and recovery studies. Conventional histopathological examinations were also done to correlate the results of both the studies. Thickness of tissue samples was around 5mm. Photobleaching profiles of native fluorophores in distilled water were measured. Various combinations of native fluorophores, FAD, FMN and Protoporphyrin were studied (obtained from SIGMA chemicals) individually as well as in combination with scatterers (polystyrene balls from Bang labs, US) and absorbers (methylene blue) in a systematic manner. The size of scatterers used for these studies were 0.3μm, 0.65μm, 1.07μm. These solutions were measured in an optical cuvette of dimensions 1 cm x 1 cm x 5 cm.

Photobleaching in tissues was seen using 100mW power at the source, which drops to ≈20mw at the sample site after passing through necessary optics. Photobleaching in phantoms was generally seen using 100mW, 10mW, 20mW and 6mW power at the source. Recovery was observed in attenuated power just after photobleaching. Beam was attenuated using neutral density filters (ndf). In our experiments, usually 10% and 6% ndf are used, as appreciable recovery was obtained with such attenuation.

Details of the compounds used for phantom studies are given below:

1. Compound Name: Flavin Adenine Dinucleotide (FAD)
   Formula Weight: 829.5
2. Compound Name: Flavin Mononucleotide (FMN)
   Formula Weight: 478.3
3. Compound Name: Protoporphyrin IX
   Formula Weight: 606.6
4. Scatterers: Polystyrene balls of three sizes 0.3μm, 0.65μm, and 1.07μm.

3.3 Results and Discussions

Section A:

It has been observed that the autofluorescence intensity of human breast tissues gradually decreases with time during continuous exposure to laser light at 488nm. The same effect is observed in other types of tissues also e.g. skin tissue, parotid gland tissued etc. [5,6]. This temporal decrease of fluorescence signal is normally referred to as photobleaching process. Appreciable recovery has also been observed in tissues just after photobleaching while monitoring with attenuated power. Recovery is observed after bleaching the samples till steady state is achieved. In this study, fluorescence photobleaching recovery (FPR) experiments are carried out on human breast tissues in vitro at emission wavelengths 530nm and 630nm as a function of different illumination intensities and different exposure times. The two emission wavelengths are chosen so as to compare FPR studies in tissues with flavins and porphyrins, the two major emitting species present in the tissues. Fig. 3.1 shows the photobleaching profiles of normal and malignant tissues at emission wavelength 530nm. The autofluorescence decay trends versus two different illumination intensities have been displayed in Fig.3.2. As can been seen, the decay profiles are dependent on exposure intensity, the rate of photobleaching increasing with increasing intensity.

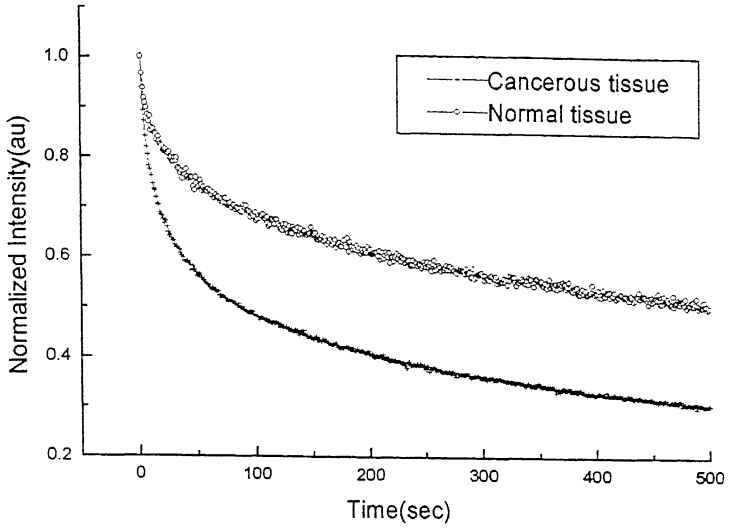

Figure 3.1 Comparison of Photobleaching rates of decay rates of Normal and Cancerous tissues at 530nm.

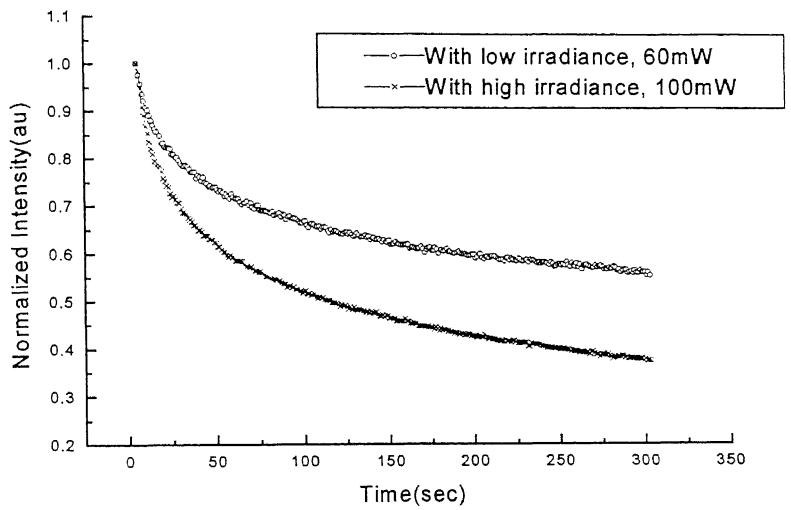

.Figure 3.2 Power dependence of tissue decay rates at 530nm.

The fluorescence decay profiles illustrates that the decay of both normal and malignant tissues follow double exponential behaviour as seen on fitting with $I(t) = A_o + A_1\exp(-(t-t_o)/\tau_1) + A_2\exp(-(t-t_o)/\tau_2)$ with a fast process (second term) and slow process (third term). The time constants (τ_1, τ_2) of the two processes differ nearly by an order of

magnitude. Constant parameters A_o, A_1, and A_2 are normalized to satisfy the condition that I(t) = 1 at t= 0, and $A_o + A_1 + A_2 = 1$. As seen in Fig. 3.1, malignant tissues decay faster than the corresponding normal tissues. This is clearly observed in the slower process τ_2. The results for both fast process τ_1 and slow process τ_2 in normal and malignant tissues are listed in table 3.1.

Table 3.1: Photobleaching decay rates for Normal and Cancerous tissues at $\lambda_{em} = 530nm$

Samples	τ_1(sec)		τ_2(sec)	
	Cancerous	Normal	Cancerous	Normal
Sample I	7	10	200	253
Samples II	11	12	104	135
Sample III	12	16	107	136
Sample IV	10	10	104	143
Sample V	9	27	132	186
Sample VI	15	17	227	262
Sample VII	35	37	296	321
Sample VIII	7	10	250	350
Sample IX	4	9	97	142
Sample X	11	12	108	161

Fig.3.3 shows the recovery at 530nm just after photobleaching while monitoring with attenuated power. The recovery profiles follow single exponential growth behavior with rate τ. The results for recovery growth rates for both normal and malignant tissues are listed in Table 3.2. As can be seen from the table 3.2, the recovery rate is higher in normal as compared to the cancerous ones.

Table 3.2: Recovery rates for Normal and Cancerous tissues at λ_{em} = 530nm

Samples	τ(sec)	τ(sec)
	Cancerous	Normal
SampleI	70	10
SampleII	35	13
SampleIII	7	3
SampleIV	73	68
SampleV	63	3
SampleVI	15	7
SampleVII	37	No recovery

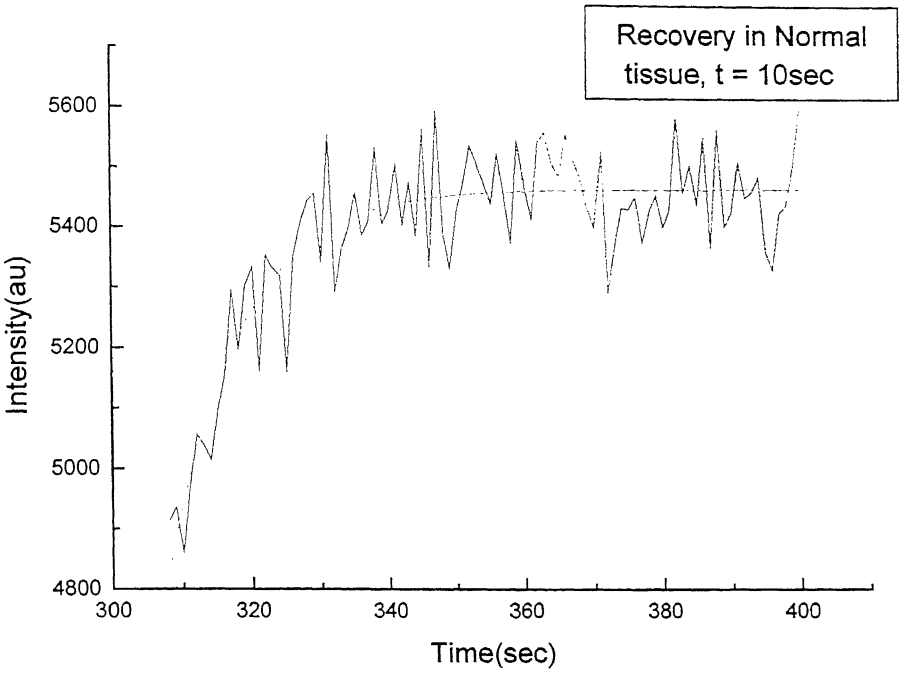

Figure 3.3 (a) FPR of normal tissue at 530nm

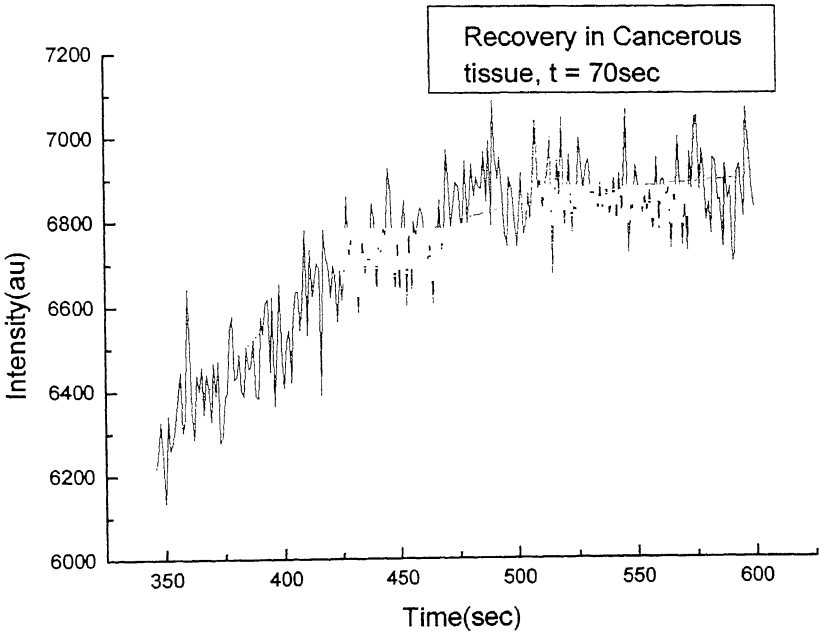

Figure 3.3 (b) FPR of cancerous tissue at 530nm.

FPR is also monitored at 630nm emission wavelength. In the limited number of samples studied, it is observed that recovery rates at 630nm are considerably slower as compared to the recovery rates at 530nm (Fig. 3.4)

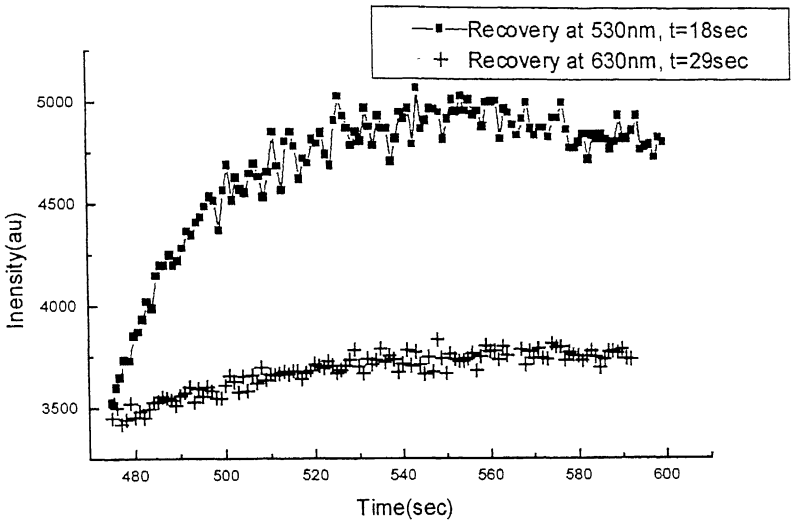

Figure 3.4 Comparison of tissue recovery rates at 630nm and 530nm for normal tissues

To obtain quantitative evaluation of temporal dynamics of photobleaching recovery processes so as to reveal information about the accumulation of different concentration of fluorophores present in the two different tissues system, studies are performed with various combinations of fluorophores, scatterers and absorbers. Photobleaching from phantoms of pure flavins and protoporphyrins are recorded and show single exponential profiles with τ = 5sec and τ = 45sec respectively as shown in Fig.3.5. A mixture of two fluorophores fitted to a double exponential with τ_1 = 10sec and τ_2 = 145sec (Fig.3.6) which suggests the presence of at least two fluorophores in the tissue.

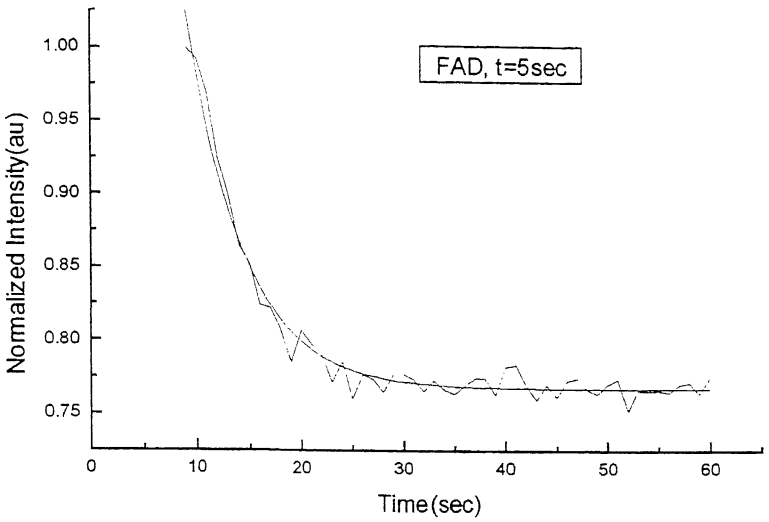

Figure 3.5(a) Photobleaching decay rate of FAD at $\lambda = 530$nm

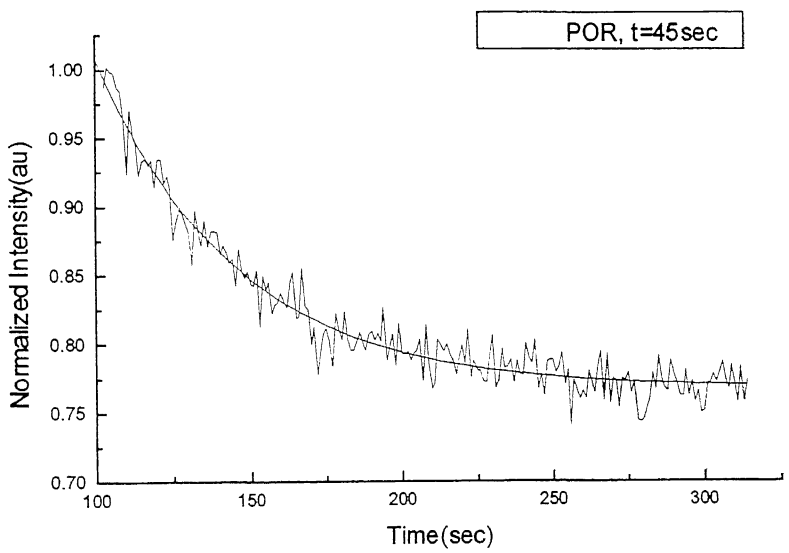

Figure 3.5(b) Photobleaching decay rate of Protoporphyrin at $\lambda = 530$nm

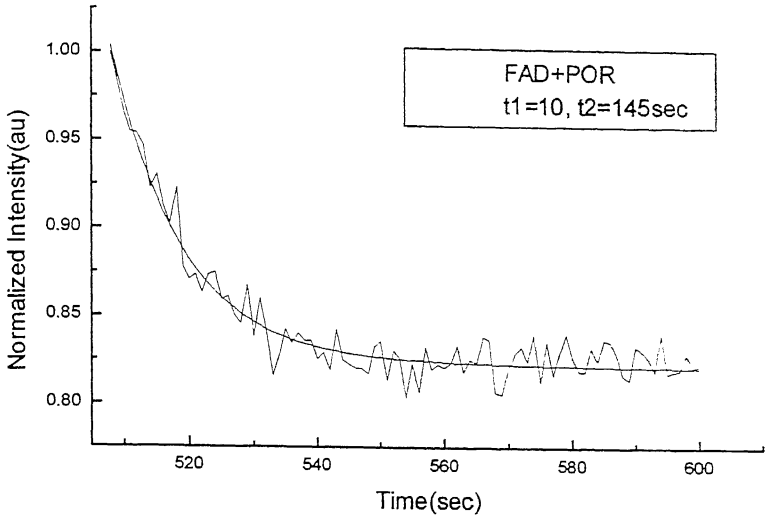

Figure 3.6 Photobleaching of FAD+Porphyrin at λ = 530nm.

It has been also observed that at particular concentrations of porphyrins and FAD, the decay profile of the solution is similar to the decay profile of tissue, which again reveals their presence in the tissues (Fig.3.6). Power dependence has also been noticed in FAD in solution as can be seen in table3.3 and figure 3.7. Figure 3.7 shows bleaching to be very fast for 100mW and is for a very short time after which recovery occurs (not shown in figure). It has been observed that for higher powers $\geq$ 100mW, bleaching is very fast and also occurs for a very short time. It can be accounted for, since bleaching occurs very fast and there is strong bleaching, the effect of molecules diffusing into the illuminated region in appreciable and occurs immediately after bleaching. However, recovery for bleaching at 10mW and 6mW are almost negligible. Thus, the optimum power to study FPR appears above 60mW.

Table 3.3 Power dependence of FAD in solution to study photobleaching decay rates at λ_{em} = 530nm.

Samples	τ(sec)	Power (mW)
25μM FAD	1	100
25μM FAD	6	10
25μM FAD	10	6

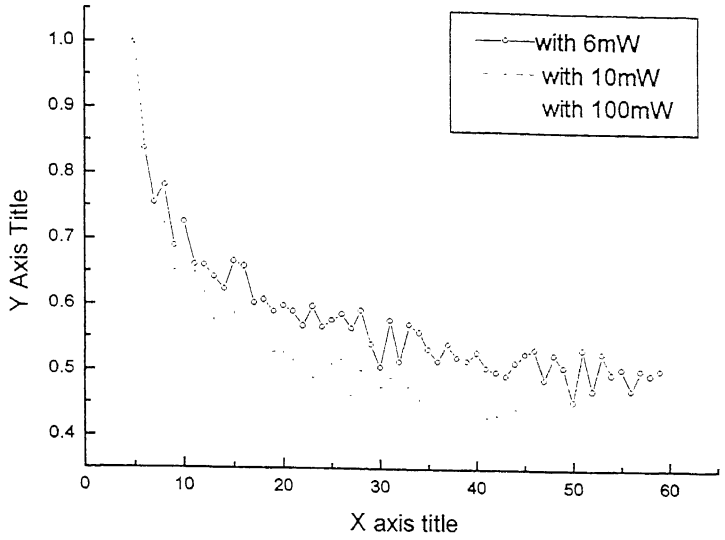

Figure 3.7 Power dependence of FAD in solution decay rates at 530nm.

Addition of scatterers to FAD solution slows down the decay rate and on adding absorber the decay rate becomes faster (table 3.4) as can be seen in Fig. 3.8 and Fig.3.9. The same phenomenon is observed in tissues containing blood, which is also an absorber. Tissues with blood are found to decay faster as compared to the tissues without any visible signs of blood. Hence, the presence of blood or any absorber enhances the decay rate in tissues and solutions. The fact that addition of absorbers increase photobleaching decay rates, indicates that the faster rate of tumor may be due to more absorption of flavin fluorescence by porphyrins. The decay rates in tissues are much slower than the decay rates in phantoms, which may be attributed to the presence of cell membrane in cells of tissues, which controls the flow of fluorophores across it.

Table 3.4: Photobleaching decay rates for phantoms at λ_{em} = 530nm

Samples	τ_1(sec)	τ_2(sec)
FAD	5	-
FAD + scatterer	12	-
FAD + absorber	2.5	19
FMN	3	65
FMN + scatterer	13	-
FMN + scatterer + absorber	3	38

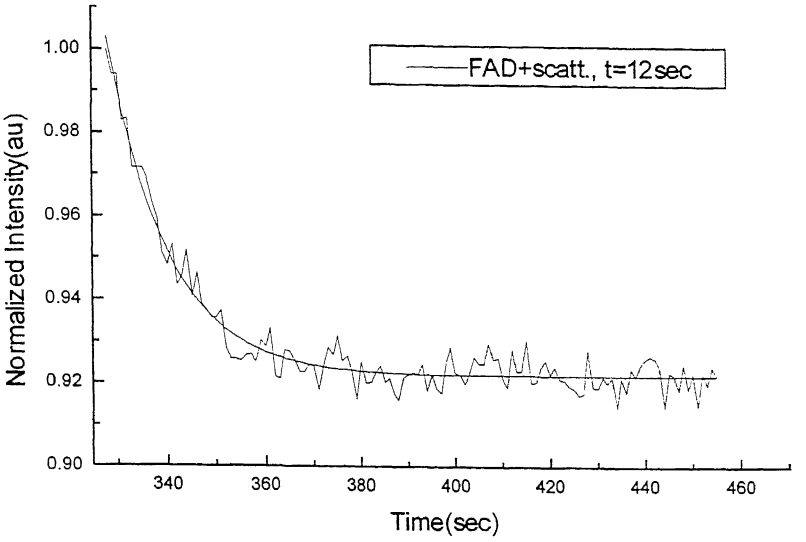

Figure 3.8 Photobleaching decay rate of FAD+Scatt. at λ = 530nm.

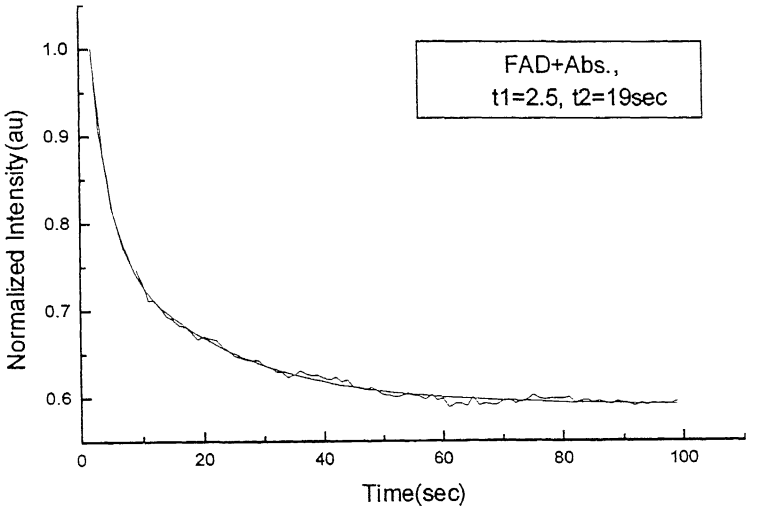

Figure 3.9 Photobleaching decay rate of FAD+ Abs. at λ = 530nm.

Recovery is also observed in phantom solutions, as shown in Fig. 3.10. Again, there is a difference in growth rates for pure FAD, FAD + scatterer and FAD + absorber (shown in table 3.5). The recovery rates become slower on adding scatterer and faster on adding absorber. So, it is possible that at a particular concentration of scatterer, absorber in phantom solution, the growth profile will exactly mimic the tissue. So, FPR studies are useful in exploring the morphology of different human tissues and looking into various photo induced chemical reactions occurring inside it.

Table 3.5: Recovery rates for Phantom solutions at λ_{em} = 530nm

Samples	τ(sec)
FAD	6
FAD +scatterer	34
FMN	4
FMN+scatterer	50
FMN+absorber+scatterer	32
Protoporphyrin	16

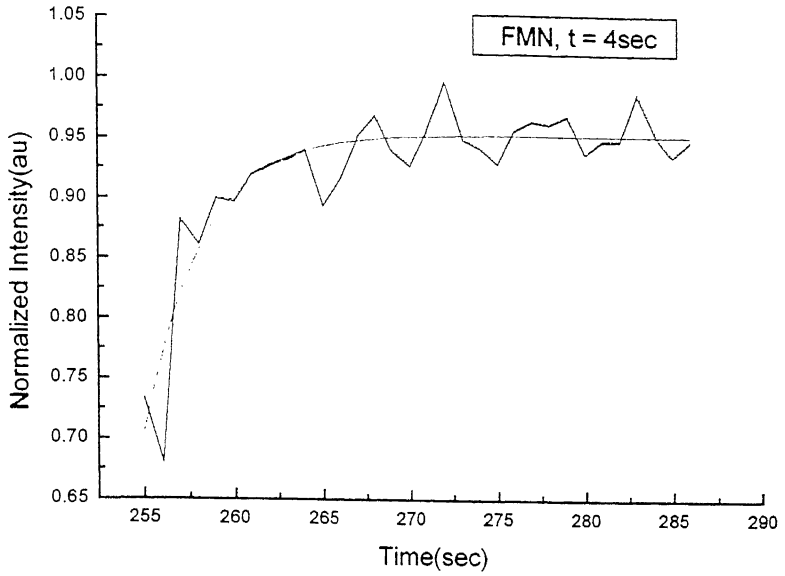

Figure3.10 (a) Recovery Rate for Pure FMN at $\lambda = 530$nm

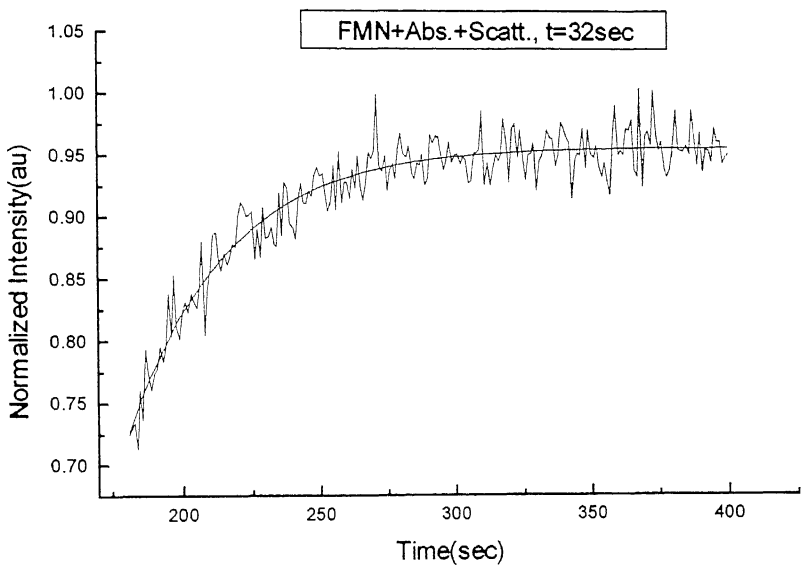

Figure3.10 (b) Recovery Rate for FMN+Scatt. +Abs. at $\lambda = 530$nm.

Further, photobleaching and recovery rates decrease as concentration of scatterers is increased with a fixed 40μM FAD (figure3.11). Table 3.6(a) and table 3.6(b) shows the photobleaching and recovery rates as the concentration of scatterers increases respectively. This may give us some information about the amount of scatterer present in normal and malignant tissues.

Table 3.6(a): Photobleaching decay rates for phantoms as scatterer concentration varies, at λ_{em} = 530nm

Samples	τ_1(sec)	τ_2(sec)
FAD + 0.5ml Scatt. (0.65μm)	2	12
FAD + 1.0ml Scatt. (0.65μm)	3	21
FAD + 1.5ml Scatt. (0.65μm)	5	46

Table 3.6(b): Recovery rates for phantoms as scatterer concentration varies, at λ_{em} = 530nm

Samples	τ(sec)
FAD + 0.5ml Scatt. (0.65μm)	13
FAD + 1.0ml Scatt. (0.65μm)	48

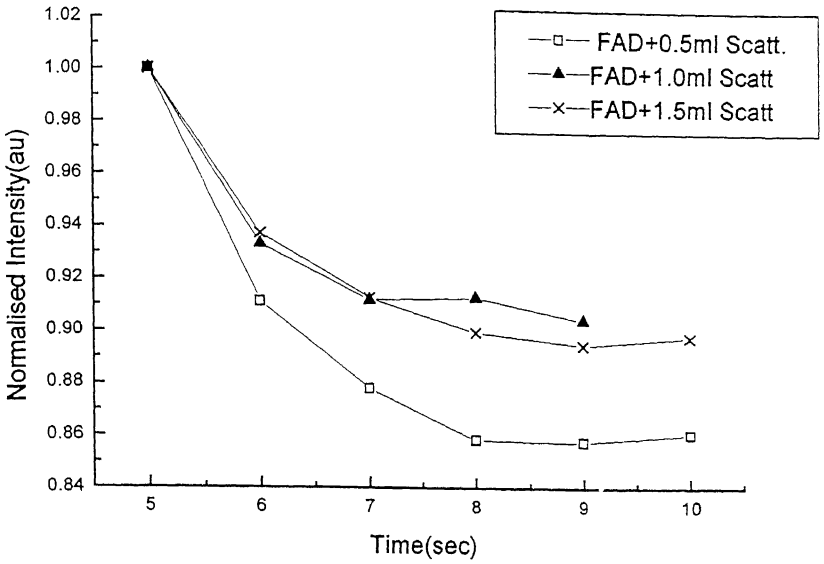

Figure 3.11 Photobleaching decay rate of FAD+ Scatt. as Scatt. concentration increases at $\lambda = 530$nm.

Photobleaching and recovery rate also decreases as scatterer size increases. It is also found that with 80μM FAD, the photobleaching behaviour was single exponential with similar rates even on adding scatterers of different sizes. This was seen in 80μM FAD with three different sizes of scatterers viz. 0.3μm, 0.65μm, 1.07μm. as can be seen in table3.7 (a) and table 3.7(b). Though there is no significant difference between the photobleaching decay rates but significant difference can be seen in the recovery rates (figure 3.12). It this appears that scatterers size plays a major role in fluorescence diffusion.

Table 3.7(a) : Photobleaching decay rates for phantoms as scatterer size varies, at λ_{em} = 530nm

Samples	τ(sec)
80μM FAD + 0.3μm Scatterer	0.7
80μM FAD + 0.65μm Scatterer	0.8
80μM FAD + 1.07μm Scatterer	1.07

Table 3.7(b): Recovery rates for phantoms as scatterer size varies, at λ_{em} = 530nm

Samples	τ(sec)
80μM FAD + 0.3μm Scatterer	3
80μM FAD + 0.65μm Scatterer	9
80μM FAD + 1.07μm Scatterer	15

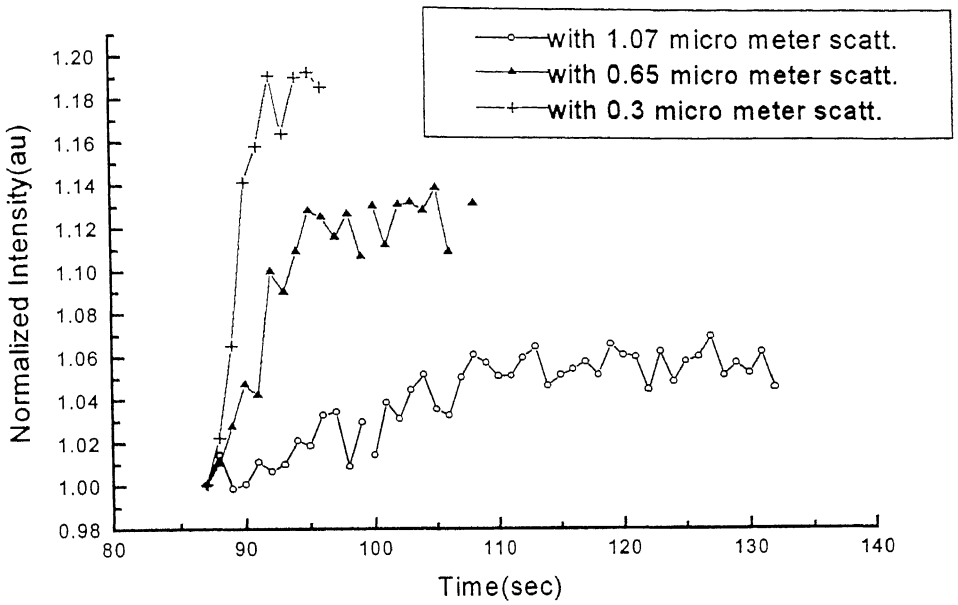

Figure 3.12 Recovery rates in pure FAD, as scatt. size varies, at λ = 530nm

Malignant tissues display slower recovery values. This may be due to the nuclear size as well as the increase in size of cell components.

To study the effect of concentration on pure fluorophore on photobleaching and recovery rates, various concentrations of pure FAD solution were studied with 100mW power at the source. Good results were not obtained for photobleaching decay rates i.e. there was no proper increase or decrease of decay rates as concentration increases. However, appreciable results are obtained when recovery is observed just after photobleaching as can be see in table3.8 (a). Same experiments were also done for various concentrations of pure FMN with 60mW power at the source. Here also recovery was observed, as given in table 3.8(b)

Table 3.8(a): Recovery rates for various concentrations of pure FAD at λ_{em} = 530nm

Samples	τ(sec)
20μM FAD	37
60μM FAD	23
80μM FAD	20
100μM FAD	4.5

Table 3.8(b): Recovery rates for various concentrations of pure FMN at λ_{em} = 530nm

Samples	τ(sec)
20μM FMN	6
60μM FMN	5
80μM FMN	4.4

From the table 3.8(a) & (b) it is clear that as concentration of pure fluorophore increases, the recovery rates become faster. However, earlier it was observed that on increasing the concentration of scatterer in pure fluorophore solution, the rate becomes slower. This can be explained as follows: the rate becomes faster on increasing the concentration of pure fluorophore in the solution. Concentration being more, fluorophores lying closer can quickly diffuse into the illuminated region.

Again, on adding scatterer the rates become slower, proving that fluorphore motion is hindered by adding scatterers. The rate of bleaching is also reduced on addition of scatterers, implying that scatterers affect the incident light falling on the fluorophores. The above results of fluorophore concentration dependence and scatterer concentration dependence indicates that recovery is more a diffusion process rather than a chemical one.

Experiments were also performed with λ_{ex} = 457.9nm and the results are compared with those obtained with λ_{ex} = 488nm, for 20μM FAD, irradiated with 100mW power at the source, as can be seen in table 3.9 and table 3.10. Experiments were done with 20μM FAD solution.

Table 3.9(a): Photobleaching decay rates for phantoms at λ_{em} = 530nm at λ_{ex} = 457.9nm

Samples	τ_1(sec)	τ_2(sec)
FAD	0.5	-
FAD +Scatt.	1	-
FAD +Scatt.+Abs.	2.5	-

Table 3.9(b): Photobleaching decay rates for phantoms at λ_{em} = 530nm at λ_{ex} = 488nm

Samples	τ_1(sec)	τ_2(sec)
FAD	1	-
FAD +Scatt.	7	-
FAD +Scatt.+Abs.	4	-

As can be seen from the table 3.9(a) & (b), the bleaching rate for pure FAD is faster at λ_{ex} = 457.9nm as compared to bleaching rates at λ_{ex} = 488nm. Power dependence can also be noticed at both the excitation wavelengths. Same is true for FAD + scatterer, decay rates are faster at λ_{ex} = 457.9nm as compared with λ_{ex} = 488nm. Again, for FAD+scatterer

+absorber, the decay rates at λ_{ex} = 457.9nm as compared to bleaching rates at λ_{ex}= 488nm is also faster.

Recovery was also seen in FAD solution as given in table 3.10 (a) & (b)

Table 3.10(a): Recovery rates for phantoms at λ_{em} = 530nm at λ_{ex} = 457.9nm

Samples	τ(sec)
FAD	1
FAD +Scatt.	No recovery
FAD +Scatt.+Abs.	3.5

Table 3.10(b): Recovery rates for phantoms at λ_{em} = 530nm at λ_{ex} = 488nm

Samples	τ(sec)
FAD	2
FAD +Scatt.	31
FAD +Scatt.+Abs.	7

Again from the table, it can be seen that recovery rate is faster for FAD, FAD+scatterer+absorber at λ_{ex} = 457.9nm as compared to recovery rates at λ_{ex} = 488nm. From the above results it may be concluded that photobleaching and recovery at 488nm excitation provides a distinct changes in rates on adding scatterers and absorbers i.e. environmental effects are more prominent with 488nm excitation. This may be due to the fact that porphyrin may be contributing to the emission process at this excitation wavelength.

Generally, photobleaching is observed at higher powers while recovery is seen with attenuated power. However, opposite is observed in Protoporphyrins in solution. It is observed that the porphyrin solution does not bleach at high power. Instead, it bleaches with attenuated power. This change may be accounted for the opening of Protoporphyrin

ring structure molecule and formation of some other photoproducts [7]. It should be noted here that the tissues monitored at 630nm do not show such a phenomenon. Thus, in tissues, porphyrins may be in an environment where such photoproducts may not be produced.

Section B:

As said earlier FPR experiments can also be used to calculate the fraction of mobile fluorophores by calculating fractional recovery and diffusion rates. A small region of a surface containing mobile fluorescent molecules is exposed to a brief intense pulse of light, thereby causing irreversible photochemical bleaching of the fluorophore in that region. Transport coefficients (e.g. Diffusion coefficients) are determined by measuring the rate of recovery of fluorescence, which results from the transport of fluorophores into the bleached region from unirradiated parts of the medium. The mathematical expression of fractional recovery, fraction of total fluorophores, which is mobile, and diffusion coefficient [1] is given as:

Fractional Recovery is defined as

$$f_K(t) = \frac{F_K(t) - F_K(0)}{F_K(\infty) - F_K(0)} \qquad 1)$$

where $F_K(t)$ is the fluorescence at any time after bleaching

$F_K(0)$ is the initial fluorescence after bleaching

$F_K(\infty)$ is the constant fluorescence intensity achieved during recovery after a long time

If some of the fluorophores in the illuminated region are immobile, the asymptote of the fluorescence recovery after bleaching, $F_K(\infty)$ will be less than $F_K(-\infty)$. Then the fraction of total fluorophores, which is mobile, is given by

$$(F_K(\infty) - F_K(0)) / (F_K(-\infty) - F_K(0)) \qquad 2)$$

where $F_K(-\infty)$ is the fluorescence before bleaching.

The diffusion coefficient is given by

$$D = (\omega^2/4\tau_{1/2})\gamma_D \qquad 3)$$

where ω is the spot size of focused laser beam

$\tau_{1/2}$ is the time for which $f_K(\tau_{1/2}) = ½$

$\gamma_D \equiv \tau_{1/2}/\tau_D$ and for circular beams $\gamma_D = 0.88$

$\tau_D \equiv \omega^2/4D$ is the characteristic diffusion time.

The above mathematical equations is based on the assumption that laser beam is single, circularly symmetric, focused laser beam for both bleaching and, appropriately attenuated, for observations of recovery. The values of diffusion coefficient and mobile fractional for various phantom solution and various tissue sample is given is table 3.11.

Table 3.11: Diffusion coefficients and mobile fraction for various phantom solutions and tissues samples.

Samples	τ(sec)	$\tau_{1/2}$(sec)	Mobile Fraction	D (x 10^{-11} m^2/cm)
FAD	6	3	0.81	0.73
FAD+Scatt.	34	17	0.61	0.13
FMN	2	1	0.77	2.2
FMN+Scatt.	Very small recovery	Very large value (i.e. a small recovery)	0.21	Very small value
Normal1	18	9	0.24	0.244
Cancerous1	38	19	0.16	0.116
Normal2	3	1.5	0.61	1.46
Cancerous	63	31.5	0.53	0.069

As can be seen from the table 3.11, the value of mobile fraction is more for pure FAD as compared to that of FAD+Scatt., which implies that scatterers hinder the mobility. Comparing the studies with tissues, it can be seen that number of mobile fluorophores are more in normal tissues as compared to the cancerous one, which can be a direct indication of higher concentration of scatterer in cancerous tissues. Also, the value of mobile fraction is less in tissues as compared to pure phantom solution, which accounts for the presence of scatterers and absorbers in the tissue. So, from the results we can characterize tissue media to be turbid and dense medium and distinguish different types by this.

3.4 References

1. D. Axelrod, D.E. Koppel, J.Schlessinger, E.Elson, W.W.Webb, mobility measurements by analysis of fluorescence photobleaching recovery kinetics, Biophys. J.16: 1055-1068 (1976).

2. Teck-Chee, Chia, Zhiwei Huang, Wei Zhang, Cheong-Houng Diong, F Seow Choen, Changes in autofluorescence emission intensities of human colonic tissues due to photobleaching process, SPIE Vol.3568 (1998).

3. Alexander A.Stratonnikov, Vladimir S. Polikarpov, Victor B.Loschenov, Photobleaching of Endogenous Flourochromes in Tissues in vivo during laser irradiation, SPIE Vol. 4241, 13-24 (2000).

4. Juan Yugerabide, Jeffrey A. Schmidth, Evangelina E. Yugerabide, Lateral Mobility in membranes as detected by fluorescence after photobleaching. Biophys. J. 39: 69-75 (1982).

5. H.Zeng, C.MacAulay, B.Palcic, D.I.Mclean, Laser induced changes in autofluorescence of in vivo skin, SPIE Vol.1882, 278-290 (1993).

6. L.Grossweiner, light dosimetry model photodynamic therapy treatment planning, Laser Sur. Med. 11: 165-173 (1991).

7. R.Rotomskis, S.Bagdonas, G.Streckyte, Spectroscopic studies of photobleaching and photoproduct formation of porphyrins used in tumor therapy. Photochem. Photobio. B 33: 61-67 (1996).

CHAPTER 4

Theoretical Modeling of Photobleaching and Recovery

4.1 Introduction

The photobleaching phenomena have been well studied for exogenous fluorophores used in photodynamic therapy (PDT)[1]. The photobleaching control of exogenous fluorophores during PDT may serve as a dose metric because destruction of fluorophores may be correlated with tissue damage. The photobleaching studies during PDT are important also for evaluating the optimal relation between fluorophore concentration in tissues and light dose applied in treatment. It is clear that for easily photobleached fluorophores their low concentration in tumor tissue cannot be compensated by high light dose as fluorophores can be fully destroyed in this case. The optimal fluorophores concentration for tumor tissue is that it could provide the lethal dose of radicals before the complete photobleaching takes place but for normal tissue the fluorophores should have complete photobleaching before such radical dose will be attained. Here, we have tried to develop model for photobleaching and recovery and to use study the kinetics of the fluorophores in the tissues. Optimization of fluorphore concentration in tumors is essential since photobleaching plays a vital role in reducing the effects of radical formation.

4.2 Photobleaching models

Attempts have been made to propose a mathematical model for photo bleaching and recovery. One such model was given by A. A. Stratonnikov et al. [2]. Photobleaching in tissues is a phenomena where fluorophores fluorescence decreases in time during irradiation with visible excitation. This is most probably due to the destruction of the fluophores and hence implies a decrease in concentration.

The destruction of fluorophores in general is described by the following equation:

$$\frac{d[C]}{dt} = -k[C][R] \qquad (1)$$

where t is time, [C] is fluorophores concentration, k is rate constant and [R] is the concentration of active agents inducing fluorophores destruction. If the destruction of fluorophores is due to its direct interaction with photons then the photons also may be considered here as the active agents. The active agents here may also be different photoproducts resulting from the interaction of light with fluorophores itself or other substances present in the tissue. The concentration of these agents can be written in the form:

$$[R] \sim [R_o] + k_1[R] \qquad (2)$$

where the first term is responsible for the active agents independent from fluorophores concentration while the second term is proportional to fluorophores concentration and is due the interaction of light activated fluorophores with other substances (singlet oxygen formation during photodynamic therapy) [R]. Using equations (1) and (2), bleaching kinetics is given by:

$$\frac{d[C]}{dt} = \frac{-1}{\tau_1} C - \frac{1}{\tau_2 C(0)} C^2 \qquad (3)$$

In this equation the values of τ_1 and τ_2 are the time constants for the first and second order bleaching correspondingly and C(0) is the value of C at t = 0.

In equation (3) the first term is linear in C(concentration) and arises when photobleaching or fluorophore destruction is due to the interaction of tissue with direct photons and

bleaching is first order. The second term is quadratic in C, which arises when second order bleaching takes place i.e. here the fluorphore destruction is due to its interaction with photoproducts generated by the bleaching of the fluorophore itself. It is assumed that for many fluorophores used in photodynamic therapy the singlet oxygen produced is responsible for the destruction.

The solution of equation (3) has the following form

$$\frac{C(t)}{C(0)} = \frac{\exp(-t/\tau_1)}{1+\frac{\tau_1}{\tau_2}[1-\exp(-t/\tau_1)]}$$

It can be easily seen that in two limiting cases of the first order bleaching ($\tau_2 \to \infty$), and second order bleaching ($\tau_1 \to \infty$), this relation reduces to the well known equations

$$\frac{C(t)}{C(0)} = \exp(-t/\tau_1) \qquad \text{first order bleaching } (\tau_2 \to \infty)$$

$$\frac{C(t)}{C(0)} = \frac{1}{(1+t/\tau_2)} \qquad \text{second order bleaching } (\tau_1 \to \infty)$$

4.3 Fluorophore kinetics

The above written relations for bleaching kinetics are valid only for spatially homogeneous light distribution in a sample. When one observes photobleaching in tissue irradiating it from the surface and measuring escaping fluorescence the problem is spatially not homogeneous. Light intensity decreases with tissue depth and destruction rate of fluorophore near the surface will be higher than deeper down within the tissue. The escape probability of fluorescence photons also decreases with the tissue depth. So the fluorescence signal measured at the surface is averaged through some tissue depth. This averaging results in lower fluorescence decrease rate compared to that in the upper surface layer. A simple model based on the above concentration dependent equation is discussed below.

Consider a homogeneous semi-infinite tissue sample irradiated from the surface by a wide beam so the problem is one dimensional. The light intensity inside the tissue decreases exponentially into a depth so that:

$$P(z) = P(0)\exp(-z/\delta_x)\,, \tag{1}$$

where P(0) is the light power density in the upper tissue layer and δ_x is the light penetration depth which depends on the wavelength of the incident (excitation) light. It should be noted that due to the back-scattered flow, the light intensity in the upper tissue layer may be several times higher than that incident on the surface of the tissue. The escape probability of a fluorescence photon from the depth z to the surface of the tissue is also described by an exponential function:

$$G(z) = G(0)\exp(-z/\delta_m) \tag{2}$$

where δ_m is light penetration depth at the wavelength of fluorescence emission. The fluorescence signal intensity measured at the surface can be written as

$$I = \int_0^\infty P(z).\sigma q C(z).G(z)dz = P(0).\sigma q.G(0).\int_0^\infty C(z).exp(-z/\delta_x).exp(-z/\delta m)dz \tag{3}$$

where σ is the absorption cross section and q is the fluorescence quantum yield. The dependence of fluorophore concentration on time and depth, C(t,z) is obtained by solving the above integral in terms of intensity. Substituting the values of P(z) and G(z) from equation (1) and (2) in equation (3), we get

$$I = P(0).\sigma q.G(0).\int_0^\infty C(z).exp(-z/\delta_x).exp(-z/\delta m)dz \tag{4}$$

Stratonnikov et. al used the values of C(t,z) from previous section in above equation and under limiting conditions, solved the above integral. Secondly, their mathematical model is only for photobleaching process. Here, a more genuine mathematical model starting from the experimental data, in which no assumption has been made, is presented. Moreover, this model applies well to recovery process also.

$$\Rightarrow I = K \int_0^{\infty} C(t,z)\exp[-\frac{z}{\delta_x}(1+\frac{\delta_x}{\delta_m})]dz$$

where, $K = P(0).\sigma q.G(0)$

Let $p = \exp(-z/\delta_x)$

$\Rightarrow dp = \exp(-z/\delta_x)\ (-dz/\delta_x)$

$$\Rightarrow I = K \int_0^{1} C(t,z)p^{(\delta_x/\delta_m)}\delta_x dp \qquad (5)$$

Now, C(t,z) is the fluorophore concentration. As the probability of depletion is proportional to probability of penetration,

$C(t,z) = C(t\exp(-z/\delta_x)$,

Substituting this value of C(t,z) in equation (5), we get

$$\Rightarrow I = K \int_0^{1} C(t\exp(-z/\delta_x)p^{(\delta_x/\delta_m)}\delta_x dp \qquad (6)$$

Again, let $u = t\exp(-z/\delta_x)$ and $\alpha = (\delta_x/\delta_m)$

Thus, $u = tp$

and $du = tdp$

Substituting this in equation (6), we get

$$\Rightarrow I = \frac{K\delta_x}{t^{\alpha+1}} \int_0^{t} C(u)u^{\alpha}du \qquad (7)$$

$$\Rightarrow \frac{dI}{dt} = \frac{-K\delta_x(\alpha+1)}{t^{\alpha+2}} \int_0^{t} C(u)u^{\alpha}du + \frac{K\delta_x}{t^{\alpha+1}}C(t)t^{\alpha} \qquad (8)$$

$$\Rightarrow \frac{dI}{dt} = \frac{-(\alpha+1)}{t}I(t) + \frac{K\delta_x}{t}C(t)$$

$$\Rightarrow K\delta_x C(t) = t\frac{dI}{dt} + (\alpha+1)I(t) \qquad (9)$$

$$\text{or } C(t) = [t\frac{dI}{dt} + (\alpha+1)I(t)]/K\delta_x \qquad (10)$$

Now, finally, concentration dependence on excitation intensity and rate of change of excitation intensity is obtained. Photobleaching kinetcs can be studied from dC/dt vs. C plot.

For a single exponential bleaching or recovery, I varies as

$$I(t) = I_o \pm A\exp(-(t-t_o)/\tau), \text{ where } A>0 \tag{11}$$

Substituting this value of I(t) in equation (10), we get

$$C(t) = [I_O(\alpha+1) \pm A(\alpha+1-t/\tau)exp(-(t-t_O)/\tau)]/K\delta_x \tag{12}$$

The curve C(t) vs. t has minima or maxima at $t^* = (\alpha+2)\tau$ which describes the start of recovery and bleaching for bleaching and recovery respectively.

If photobleaching shows a double exponential behaviour then minimum lies between $(\alpha+2)\tau_1$ and $(\alpha+2)\tau_2$.

Finally,

$$\frac{-dC}{dt} = \pm A(\alpha+2-t/\tau)exp(-(t-t_O)/\tau)/K\tau\delta_x \tag{13}$$

$$\Rightarrow -\frac{dC}{dt} = \frac{[C - I_O(\alpha+1)/k\delta_x]}{\tau} + \frac{[C - I_O(\alpha+1)/k\delta_x]}{[\tau(\alpha+1)-t]} \tag{14}$$

which provides further information on photobleaching recovery kinetics.

Results and Discussions

For a particular excitation wavelength, emission at a certain wavelength is monitored during photobleaching recovery experiments. When excitation wavelength and emission wavelength are held constant, then δ_x/δ_m may be taken to be constant. In equation (14), it is the last term which is significant. This determines whether a particular process occurring (bleaching or recovery) will dominate or compete. At $t\rightarrow\infty$, from equation (12),

$C(t) = \frac{(\alpha+1)I_O}{K\delta_x}$, which is a constant or a steady state value

Then, $[C-\frac{(\alpha+1)I_o}{K\delta_x}]$ will always be positive for photobleaching. Now, whether the process will boost or compete will be determined by the curvature of C(t) vs t profile. The maxima or minima occurs at $t^* = (\alpha+2)\tau$. Therefore , $(\alpha+1)\tau$ will be less than t^*. Now, from equation (14) at any time $(\alpha+1)\tau > t$, the last term will be postive and so the process going on will dominate. If $(\alpha+1)\tau < t$, the other process will compete and dominate. Hence, starting with photobleaching there will increase in concentration after it has achieved minima at $t^* = (\alpha+2)\tau$, leading to observation of increase in the fluorescence intensity at a later time.

Now, again for $(t-t_o)/\tau \ll 1$, C is a linear function of time and it is of first order kinetics case and also for very long time scale it becomes first order kinetics differing from the earlier situation by a constant. But, for intermediate time scales higher powers of C can come from expansion, signifying the presence of many higher order kinetics terms depending on the situation.

$\frac{dC}{dt}$ vs C describes how the slope is changing with C(t). Maximum change will occur when $\frac{d^2C}{dt^2} = 0$ i.e. when $t^{\sim} = (\alpha+3)\tau$ which again determines whether the process will dominate or compete. So, we have the behaviour of C(t) r in the region $1 \ll (t-t_o)/\tau \ll 1$ and around the minima $t^* = (\alpha+2)\tau$. Complete behaviour can be extrapolated and our ideal profile should be as the relative concentration profile shown for 20μM FAD in figure 4.1(b). Figure 4.1(a) is the bleaching profile of FAD from which figure 4.1(b) is deduced.

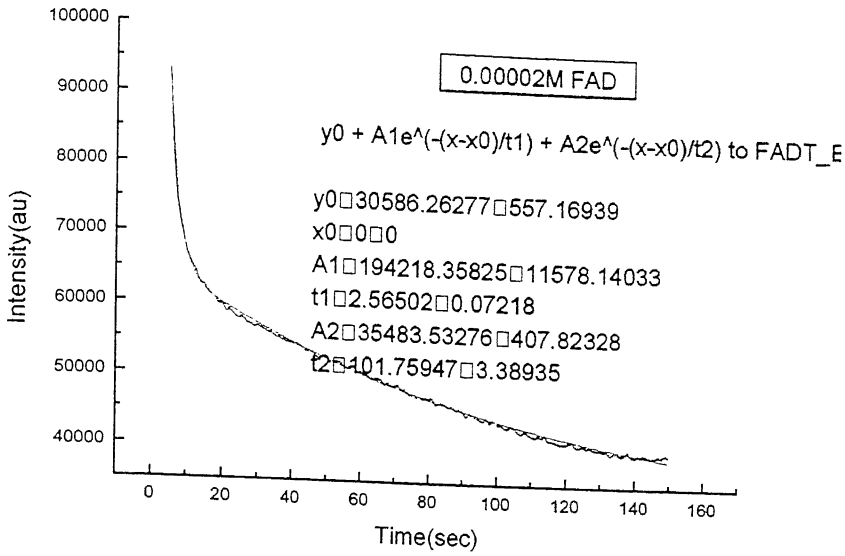

Figure 4.1(a): Photobleaching decay profile of 20μM FAD at λ_{em} = 530nm

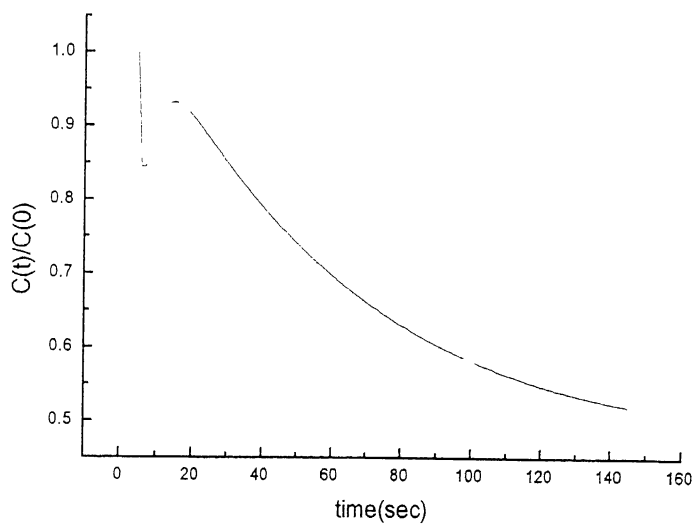

Figure 4.1(b): Relative concentration profile for 20μM FAD

This means that there are two competing process always occurring, with one dominant at a time. Figure 4.2(a) shows the recovery in 100μM FAD with growth rate τ = 53sec. Figure 4.2(b) shows the corresponding C(t)/C(0) vs t profile and it is found from the graph that minima occurs at $t^* = 137\text{sec} \approx (\alpha+2)\tau$ above which photobleaching starts dominating. Hence our experimental observations satisfies the mathematical model.

Again from figure 4.2(c), which is the deduced dC/dt vs t plot of figure 4.2(a), the minima occurs at $\tilde{t} \approx (\alpha+3)\tau$, as expected from the model. Similar results are obtained from 60μM FAD [figure 4.3 (a),(b),(c)], confirming the significance of the model.

Now, taking the 2nd derivative,

$$\frac{d^2C}{dt^2} = \frac{-\tau[\alpha+3-t/\tau]}{[\alpha+2-t/\tau]} \qquad (15)$$

If $t < (\alpha+2)\tau$, then equation (15) will not change its sign and hence the process will boost. However, if $(\alpha+2)\tau < t < (\alpha+3)\tau$, then the process will compete.
Hence three points that determines the kinetics are $t = (\alpha+1)\tau$, $t^* = (\alpha+2)\tau$ and $\tilde{t} = (\alpha+3)\tau$.

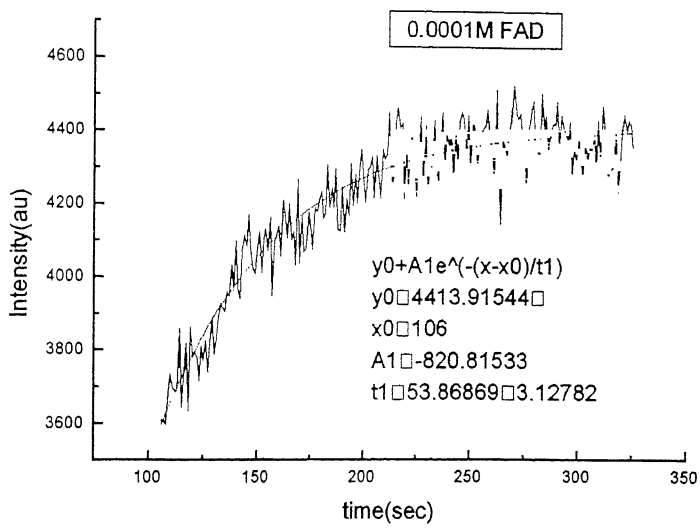

Figure 4.2(a): Photobleaching decay profile of 100μM FAD at λ_{em} = 530nm

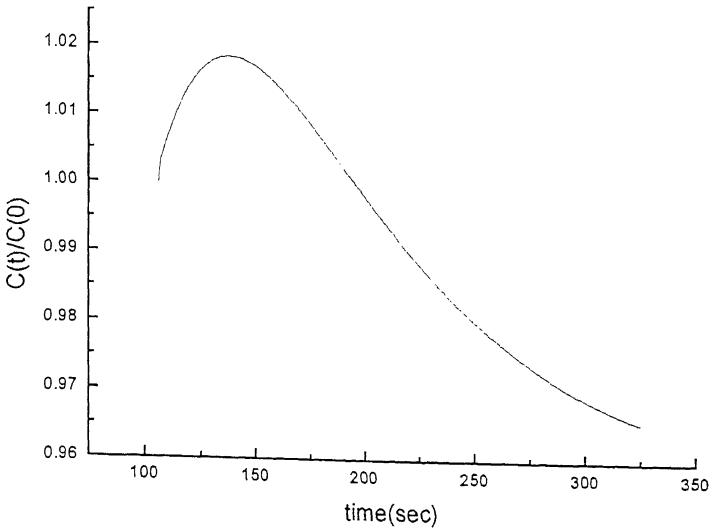

Figure 4.2(b): Relative concentration profile for 100μM FAD

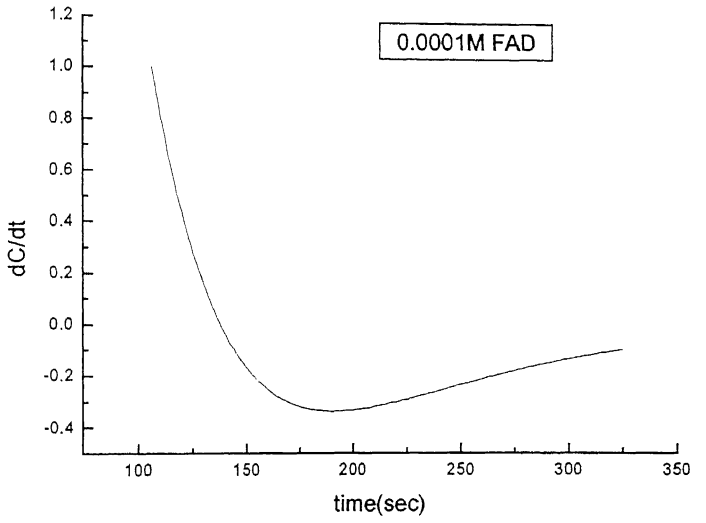

Figure 4.2(c): dC/dt vs t profile for 100μM FAD

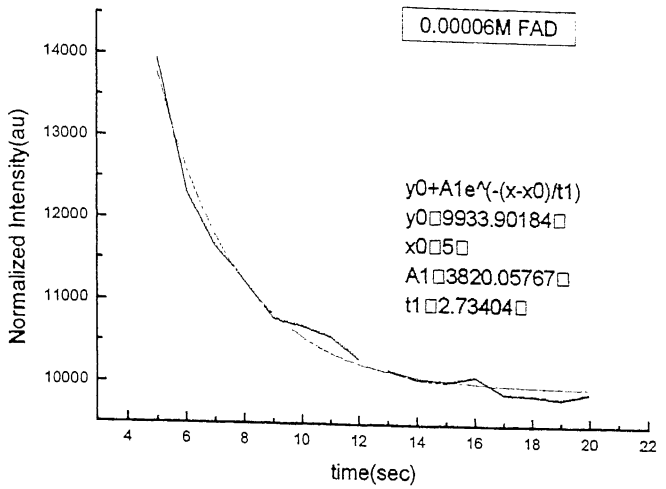

Figure 4.3(a): Photobleaching decay profile of 60μM FAD at λ_{em} = 530nm

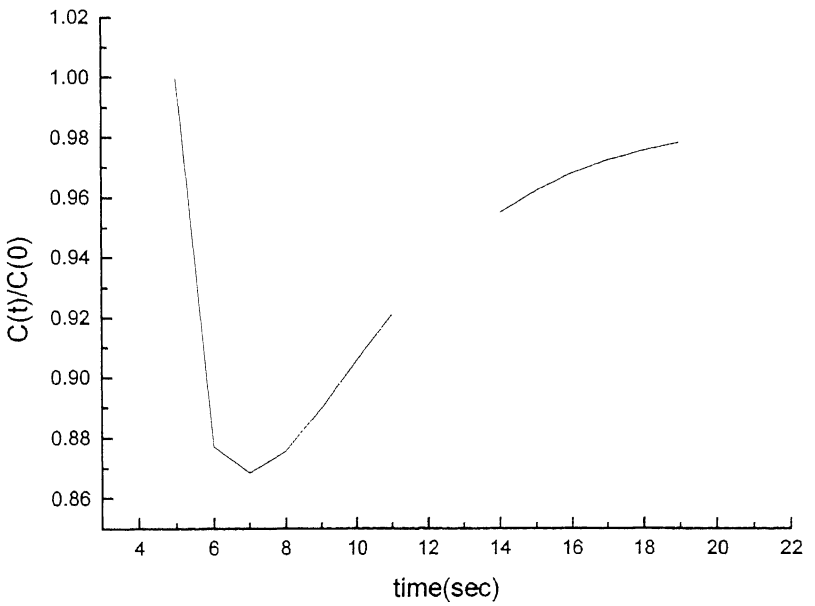

Figure 4.3(b): Relative concentration profile for 60μM FAD

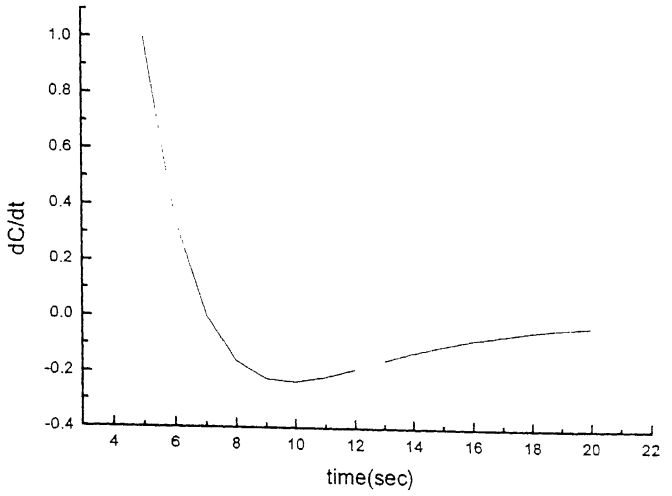

Figure 4.3(c): dC/dt vs t profile for 100μM FAD

Figure 4.4 shows the C(t) vs. t profile for 20μM FAD and 80μM FAD with recovery rates τ = 35sec and 18sec respectively. As the recovery rate is faster for 80μM FAD, it attains maxima earlier than 20μM FAD as $t^* = \tau(\alpha+2)$.

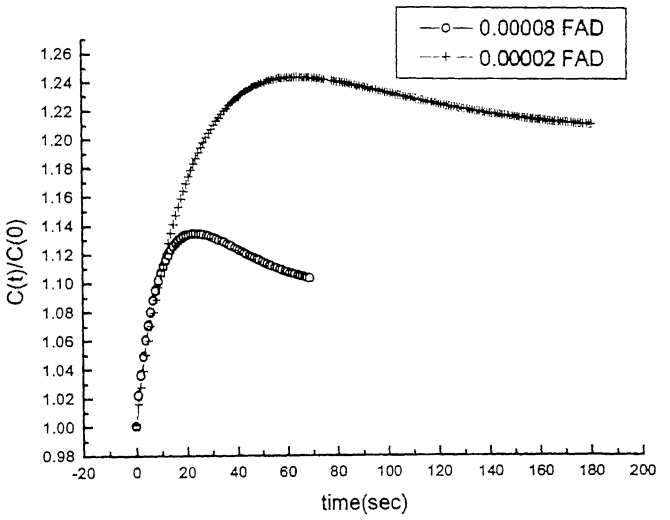

Figure 4.4: Comparison of relative concentration profile for recovery in 20μM FAD and 80μM FAD

Further, on adding absorber to FAD, σ changes and δ_x/δ_m changes and therefore there is difference in the C(t) vs. t profile for all three as can been seen in figure 4.5(b). On adding scatterer and absorber, the intensity profile follows double exponential behaviour. On adding absorber the rate becomes faster and hence the first minima $(\alpha+2)\tau_1$ shifts slightly to left as compared to minima of pure FAD. On the other hand, on adding scatterer to the pure FAD solution, the rate becomes slower and hence the first minima $(\alpha+2)\tau_1$ shifts to right as compared to the minima of pure FAD solution as can be seen in figure 5(b). figure4.5(a) shows the photobleaching profiles of three solutions viz. FAD, FAD+scatterer, FAD+absorber with τ = 6sec, 9sec and 2.5sec respectively.

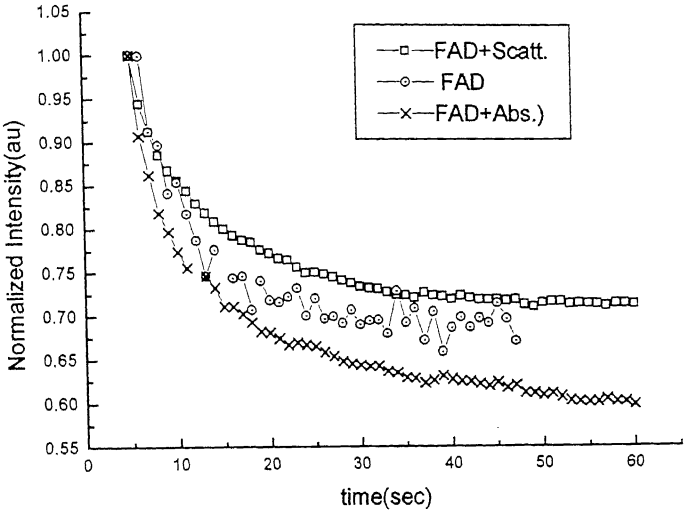

Figure 4.5(a): Comparison of photobleaching decay profiles of FAD, FAD+Scatt., FAD+Abs. at λ =530nm

Phantoms studies were then correlated with tissue dynamics. In tissues, intensity decay profile is double exponential behaviour. Hence, then minima should lie between $\tau_1(\alpha+2)$ and $\tau_2(\alpha+2)$ as can be seen in figure 4.6. The slower and faster decay rates (t_1, t_2) sec of cancerous and Normal human breast tissue are (10, 103) sec and (11,130) respectively. The minima for cancerous tissues occurs at $t^* \approx 210$sec and for normal $t^* \approx 230$sec.

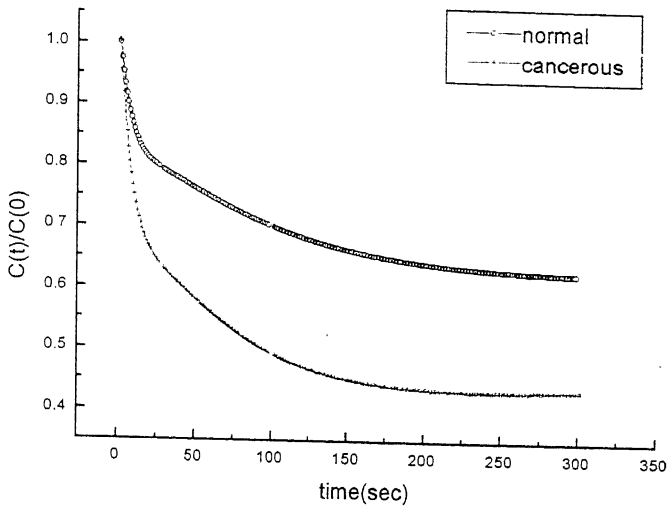

Figure 4.6 Comparison of relative concentration profiles of Normal and Cancerous tissue

4.5 References

1. R.Rotomskis, S.Bagdonas, G.Streckyte, Spectroscopic studies of photobleaching and photoproduct formation of porphyrins used in tumor therapy. Photochem. Photobio. B 33: 61-67 (1996).

2. Alexander A.Stratonnikov, Vladimir S. Polikarpov, Victor B.Loschenov, Photobleaching of Endogenous Flourochromes in Tissues in vivo during laser irradiation, SPIE Vol. 4241, 13-24 (2000).

CHAPTER 5

Conclusion

5.1 Conclusion

The temporal dynamics of autofluorescence intensity of human breast tissues during irradiation of laser light at 488nm excitation have been determined in this thesis report. The tissues dynamics is than correlated with phantom studies. Recovery is observed in both tissues and phantom solutions. The rates of photobleaching and recovery are dependent upon the intensity of incident light and exposure time. The photobleaching decay profile of FAD + Porphyrin indicates the contribution of both the fluorophores in tissue photobleaching at 530 nm. Tumor photobleaching profiles display faster decay rates as compared to the normal. Addition of absorber increases the photobleaching decay rates while addition of scatterer slows it down. The faster decay rates of tumor tissues suggest that this may be due to absorption of flavin fluorescence by porphyrins. This indicates the higher concentration of porphyrins in tumor tissues than normal one.

Theoretical model to study photobleaching and recovery kinetics developed gave information about the relative concentration of fluorophores in normal and cancerous tissues, thereby giving information about the concentration of scatterers and absorber

present in the tissue. The changes occurring in FPR processes may be attributed to a number of processes occurring in the tissues, like the photo induced reversible chemical reaction resulting in the formation of the photoproducts and diffusion of fluorophores across the cell membrane in cells of human tissues. However, the fluorophore concentration dependence and scatterer concentration dependence, studies shows that diffusion of fluorophores into the illuminated region plays major role in recovery, rather than any chemical process.

5.2 Scope for Future Work

Knowledge of the absolute concentration of all the fluorophores present in the tissue may help us differentiate between the normal and cancerous because, these fluorophores control the metabolism of the body.

The results obtained here may help in low intensity laser therapy. There is so far, no unambiguous opinion about the mechanism of low intensity laser therapy. The reason for it is that the primary acceptors of laser irradiation in the tissue, which may stimulate the therapy effects, are still not well identified. As of now, FPR of exogenous fluorophores have been studied for optimization in PDT. However, this study on endogenous fluorophores may also be significant during optimization studies for PDT. An example of ongoing work towards clinical optical therapeutics is to increase the efficacy of Photodynamic Therapy (PDT) by enabling treatment monitoring using fiber optical probes. In this cancer treatment modality, light activated drugs produce extremely short lived cytotoxic substances. To date three parameters, molecular oxygen, light irradiance and drug concentration are identified to govern the treatment's efficacy. By controlling the local intensity online the production of cytotoxic substances can be adjusted based on the available oxygen and photosensitizer, to maximize the tumoricidal effect, while sparing normal healthy tissue. While during photodynamic therapy the active photoproduct dose is sufficiently high to result in tissue necrosis then during low intensity laser therapy this dose is much lower resulting only to stimulation of different biological processes.

The photobleaching rate of endogenous fluorophores may serve as an effective dose metric to evaluate the influence of laser irradiation on tissue during low intensity laser therapy.